Estimation of Transplanting and Harvest Dates of Rice Crops in the Philippines Using Sentinel-1 Data

ARTURO G. CAUBA JR.
June 2023

SUPERVISORS:
Dr. Roshanak Darvishzadeh
Dr. Michael Schlund

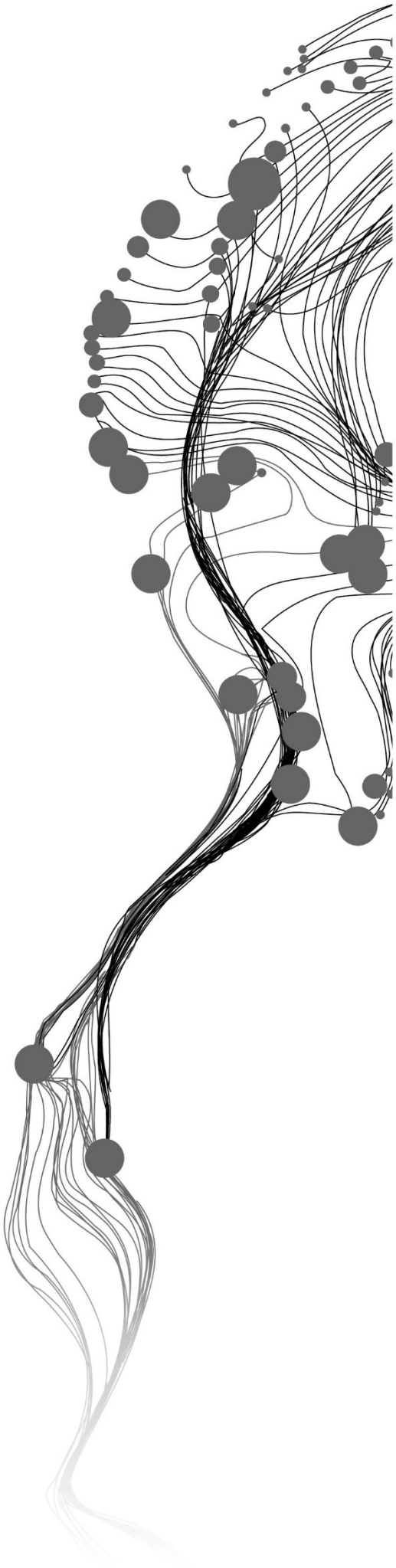

Estimation of Transplanting and Harvest Dates of Rice Crops in the Philippines Using Sentinel-1 Data

ARTURO G. CAUBA JR.
Enschede, The Netherlands, June 2023

Thesis submitted to the Faculty of Geo-Information Science and Earth Observation of the University of Twente in partial fulfilment of the requirements for the degree of Master of Science in Geo-information Science and Earth Observation.
Specialization: Natural Resources Management

SUPERVISORS:
Dr. Roshanak Darvishzadeh
Dr. Michael Schlund

THESIS ASSESSMENT BOARD:
Prof. Dr. Andy Nelson (Chair)
Dr. Alice Laborte (External Examiner, International Rice Research Institute)

DISCLAIMER

This document describes work undertaken as part of a programme of study at the Faculty of Geo-Information Science and Earth Observation of the University of Twente. All views and opinions expressed therein remain the sole responsibility of the author, and do not necessarily represent those of the Faculty.

ABSTRACT

Rice is an important staple crop in the Philippines; hence, accurate estimation of its transplanting and harvest dates is essential for efficient crop management and resource allocation. Remote sensing data, such as Sentinel-1 Synthetic Aperture Radar (SAR) data, offer valuable information for monitoring agricultural activities and predicting crop phenology. This study focused on utilizing Sentinel-1 SAR data to estimate the transplanting and harvest dates of rice crops in two distinct seasons, namely the dry and the wet seasons, in the provinces of Agusan del Sur, Cagayan, and Leyte. Transplanting and harvest dates of rice fields were obtained through farmer interviews conducted by the International Rice Research Institute (IRRI). A total of 99 rice fields were further considered (19 in Agusan del Sur, 38 in Cagayan and 42 in Leyte) in this study. Time series data from Sentinel-1A (obtained from IRRI) and Sentinel-1B (extracted from Google Earth Engine) were merged, and the mean backscatter coefficients in VV, VH, and VH/VV polarizations were extracted at the rice field level to create time series curves. The locally weighted scatterplot smoothing (LOWESS) method was applied to smoothen the time series data, and the R^2 values were used to assess the goodness of fit between the original and smoothed curves. Periodogram analysis and the Breusch-Godfrey test were employed to identify repetitive patterns and their statistical significance. Local extrema and corresponding dates were identified to indicate transplanting and harvest dates. The detected dates were then compared with those from the field survey data provided by the IRRI.

The evaluation of the goodness of fit revealed the variability of the time series data. VV polarization data during the wet season exhibited the lowest R^2 values (median $R^2 < 0.4$), with Agusan del Sur and Leyte provinces demonstrating higher variability than the Cagayan province. Conversely, VH data consistently displayed the highest R^2 values across all three provinces (median $R^2 > 0.59$), indicating stronger linear relationships between the original and LOWESS-smoothed time series curves. Around the transplanting period, the backscatter coefficients decreased, resulting in minimal backscatter. We observed some discrepancies between the transplanting dates reported by farmers and our detected dates. During the dry season, the lowest root mean squared differences (RMSD) for transplanting dates were 9.2, 16, and 13.6 days and during the wet season, were 14, 29, and 27 days in Agusan del Sur, Cagayan, and Leyte, respectively. When estimating the harvest dates, VH and VH/VV polarization consistently corresponded to the local maximum immediately after the first local minimum. In contrast, VV polarization dates were associated with either the first or second local maximum after the first local minimum. During the dry season, the lowest RMSD for harvest dates were 17.5, 16, and 16 days and during the wet season were 8, 14, and 22 days in Agusan del Sur, Cagayan, and Leyte, respectively. In a nutshell, our results revealed the potential of VH and VV polarizations for estimating transplanting and harvest dates during the dry season, while VH/VV polarization showed promising results for estimating these dates mainly during the wet season. This research has significant implications for the agricultural sector, providing opportunities to optimize crop management practices, allocate resources effectively, and support sustainable rice production.

Keywords: Rice, crop management, transplanting, harvest, Sentinel-1, SAR, time series, LOWESS, R^2, backscatter coefficient, RMSD, local minimum, local maximum

ACKNOWLEDGEMENTS

I am deeply indebted to the following individuals and organizations whose unwavering support has been instrumental in making this thesis a reality. You have been my pillars of strength, constant sources of motivation, and beacons of optimism throughout this transformative journey.

First and foremost, I express my profound gratitude to my supervisors, Dr. Roshanak Darvishzadeh and Dr. Michael Schlund, for your invaluable guidance and the opportunity to work under your supervision. I am immensely grateful for your willingness to share your extensive knowledge and expertise, which has undoubtedly shaped the outcome of this research. Your constructive feedback and timely advice have been crucial in refining and improving the quality of this thesis.

I extend sincere thanks to the chair of the thesis assessment board, Prof. Dr. Andy Nelson, for generously dedicating your time and providing invaluable comments since the research proposal defense. Your insightful feedback and constructive criticism have greatly contributed to the enhancement of this research. Additionally, I am grateful to the external examiner, Dr. Alice Laborte, for investing your time and providing profound insights during the final defense. I also express my heartfelt appreciation to Drs. Raymond Nijmeijer for your empathy, motivational reminders to stay focused on my goals, and the heartfelt advice and counsel you have bestowed upon me.

I am deeply grateful to Caraga State University for granting me study leave and to the Department of Science and Technology – Science Education Institute for awarding me a full scholarship. Your moral and financial support has been vital not only for the completion of this MSc. thesis but also for the entire journey of obtaining my MSc. degree that I embarked on two years ago.

To my support system in the Netherlands, my friends and acquaintances—Carlos, and Finn—I extend my heartfelt appreciation. Thank you for the shared time and laughter, the enjoyable parties, and the precious memories we have created together. To Enzo, thank you for welcoming me into ITC and making me feel at home. To Dennis, Archita, Aulia, Xuanya, and Cham, thank you for the moments we shared and the birthdays and special occasions we celebrated together. Despite the challenges we faced, our friendship and support for one another remained constant and solid. To Rick, thank you for everything you have done for me. And to Robbie, thank you for coming into my life. Your presence has brought joy and positivity, and your moral support has been invaluable to me.

To my family and friends in the Philippines, words cannot express my gratitude for your unwavering support, sincere wishes, and prayers for the success of my studies. To my teachers, professors, and mentors, thank you for nurturing my mind and imparting knowledge and skills that have shaped me into who I am today. And to the Almighty Father, I am forever grateful for the blessings you have showered upon me.

The journey towards obtaining my MSc. degree, especially while working on this thesis, has been far from easy. I have faced numerous challenges, starting from the difficulties caused by the Covid-19 pandemic, which disrupted travel arrangements, to the passing of my beloved grandmother during the final stages of my studies, personal heartbreak, and various other obstacles. However, despite these trials, I have managed to persevere, always seeking out the silver lining in every situation. As I approach the final destination of completing my thesis and, ultimately, obtaining my MSc. degree, I am overwhelmed with profound gratitude for all the individuals who have accompanied me on this path. You hold a special place in my heart, and I will forever cherish our connections.

TABLE OF CONTENTS

LIST OF FIGURES

LIST OF TABLES

LIST OF ABBREVIATIONS

ADS	: Agusan del Sur
BG	: Breusch-Godfrey
CGY	: Cagayan
dB	: decibel
ESA	: European Space Agency
FAO	: Food and Agriculture Organization
GEE	: Google Earth Engine
GRD	: Ground Range Detected
HD	: Harvest Date
IRRI	: International Rice Research Institute
LOWESS	: Locally Weighted Scatterplot Smoothing
LYT	: Leyte
MAD	: Median Absolute Deviation
MODIS	: Moderate Resolution Imaging Spectroradiometer
MSE	: Mean Squared Error
NDVI	: Normalized Difference Vegetation Index
R^2 or R-squared	: Coefficient of Determination
RMSD	: Root Mean Squared Differences
SAR	: Synthetic Aperture Radar
SLC	: Single Look Complex
TD	: Transplanting Date
VH	: Vertical Transmit – Horizontal Receive polarization
VV	: Vertical Transmit – Vertical Receive polarization

1. INTRODUCTION

1.1. Background

The human population is expected to reach over 9 billion in 2050 (United Nations, 2019). This high population projection is alarming as it entails more demand for food, shelter, and energy resources to sustain human existence. In 2020, nearly one in three, around 2.37 billion people, had insufficient food (FAO, 2021). Besides, healthy diets appeared out of reach due to the soaring price of nutritious food paired with persistently high levels of income inequality (FAO, 2021). This problem has intensified since the Covid-19 pandemic started. Thus, the goal of ending food insecurity remains exceptionally challenging. The number of people affected by hunger may stay the same or continue to rise if concrete actions such as sustainable production of crops are not taken to accelerate progress and deal with the drivers of food insecurity. Another concern is that the resources consumed for human survival have been overexploited and utilized unsustainably due to the competing demands that lead to the degradation of the environment and continuous scarcity of natural resources (FAO, 2017). With the degradation of the environment and growing population, producing more crops turns out to be a challenge and food shortage has become prevalent. Hence, understanding the condition of the environment to optimize crop production is vital to solving the concern of food security.

Crop production is crucial for sustaining the global population by providing essential food crops like cassava, maize, potatoes, rice, soybeans, sweet potatoes, and wheat. These crops play a vital role in meeting the dietary needs of individuals and communities worldwide. Similarly, crop production provides income to local farmers (Steffany et al., 2017) and generates employment in numerous rural communities (Schwarcz et al., 2012). Rice is considered the most valuable food crop in several countries and is the staple food of a considerable part of the world's population (Seck et al., 2012). The Philippines is one of the largest rice consumers globally, with 14.85 million metric tons of rice consumption in 2021/2022 (Statista, 2022). Hence, with the vast number of rice consumption, the Philippines imports rice regularly to resolve the country's rice deficits (Davidson, 2016). The value of rice in the country is apparent; thus, rice production must be improved to meet the food demand. However, yield-limiting and yield-reducing factors challenge the goal of increasing rice production sustainably. The viable approach is to provide accurate temporal information on crop and water management practices and optimizing the use of the limited environment and socio-economic resources (Fikriyah et al., 2019). The temporal information on rice status is also essential to simulate rice growth models used to support agronomic management to evaluate production. Furthermore, the information on when the rice crops are being planted and harvested can help deliver production inputs and provide suggestions on the suitable crop calendar to manage the impact of the changing climatic conditions (Imran et al., 2018).

The choice of planting method plays a vital role in agricultural practices, influencing crop establishment, growth, and overall productivity. Two commonly employed methods are direct seeding and transplanting. Transplanting involves raising seedlings in a separate nursery and later transferring them to the desired location (Hossain et al., 2002). Avoiding asynchronous planting is essential as it can affect crop production. A study conducted for some provinces of the Philippines revealed that high disease incidence in rice crops was linked to asynchronous planting, while synchronous planting was associated with low disease incidence (Cabunagan et al., 2001). Knowing the harvest date of rice crops can significantly impact the farmer's profit. In recent years, the market price of rice in the Philippines has fluctuated with its highest price in 2018 (Philippine Statistics Authority, 2021). This market price instability may be avoided when the government knows how much and when the rice will be harvested. Moreover, Turner et al. (2021) showed that prolonged harvest delays led to increased lodging incidence, significantly reducing the estimated yield by up to 42.5%. By considering these factors, farmers and policymakers can make informed decisions to optimize planting methods, promote synchronous planting, and effectively manage harvest timing, improving crop productivity and economic outcomes in the agricultural sector.

Examining the crop phenological stages of rice crops may help detect the transplanting and harvest dates. Monitoring rice phenology on the ground is accurate when appropriately executed but is expensive, time-consuming, and impractical on a large scale (Corcione et al., 2016). Satellite observation is suitable for studying efficiently huge rice field areas. Several spaceborne optical and microwave sensors have been

launched over the past decades, and various methods have been developed, which paved the way to a more convenient and inexpensive way of investigating the development of rice crops. Estimating of rice phenology dates has been done through the time-series data of vegetation indices derived from Landsat (Wang et al., 2015) and Moderate Resolution Imaging Spectroradiometer (MODIS) (Sakamoto et al., 2005). In the study of Suwannachatkul et al. (2014), MODIS time-series data was used to estimate rice cultivation and harvest dates. Similarly, a research work by Chumkesornkulkit et al. (2013) aimed to estimate rain-fed rice cultivation dates using MODIS NDVI data and found that the accuracy of estimating rice cultivation and harvest dates was degraded due to weather conditions in the rainy season. The NDVI data can be affected by clouds, mainly in the rainy season. Hence, the drawback of optical sensors is the inability to observe the ground surface and capture information for areas covered with clouds, as clouds typically block visible-to-near infrared sunlight. In addition, it is sensitive to varying climatic conditions (Thies & Bendix, 2011). Microwave sensors like Synthetic Aperture Radar (SAR) offer advantages over optical sensors. SAR can penetrate clouds, making it less affected by the atmosphere and weather (He et al., 2018). Being an active sensor, SAR is not dependent on sunlight and can acquire data day and night (Walls et al., 2014). Hence, this continuous imaging capability increases the likelihood of obtaining usable acquisitions.

Various studies have shown the capability of SAR data to capture information related to the morphology and phenological stages of rice crops as well as the standing water underneath the vegetation (Lopez-Sanchez et al., 2012; Vicente-Guijalba et al., 2014). Lasko et al. (2018) implemented a random forest classifier to compare the different Sentinel-1 SAR datasets at varying spatial scales and polarizations for mapping double and single paddy rice and estimate the start of the season, end of the season, and length of the rice crop season at the commune level. The result highlighted the efficiency of Sentinel-1 in mapping rice paddy and showed that VVVH10m is the most accurate dataset for rice mapping with 93.5% overall accuracy. An earlier study in the Philippines indicated that multi-temporal SAR data could detect the rice area and the start of season dates (Gutierrez et al., 2019). Similar studies were also performed by Cota et al. (2015), who investigated rice phenology based on statistical models for time-series RADARSAT-2 SAR data and Li et al. (2016), who explored the use of RADARSAT-2 full-polarimetric SAR data in rice monitoring and retrieval of rice phenology. The previous studies generally focused on mapping rice fields and estimating the rice crop season and the different phenological stages such as vegetative, reproductive and maturity phases, while detecting transplanting and harvesting periods using Sentinel-1 SAR data has not been studied yet.

SAR data has been free and accessible to the communities of researchers since the launch of the Sentinel-1 satellite in 2014, and its potential has been demonstrated for several applications in various fields (Braun, 2021). With the constellation of Sentinel-1A and 1B, the revisit time has become six days due to acquisition overlap, and with SAR sensors, the data acquisition is feasible amidst all atmospheric conditions (Torres et al., 2017). The higher revisit period (six days) is limited only to some areas such as European countries. In some regions, like the Philippines, image acquisition generally occurs every twelve days in a descending pass (ESA, 2021). Nevertheless, Sentinel-1 SAR data is freely available and shows potential for estimating rice crop transplanting and harvesting dates.

In modelling and analyzing RS time series data, the function fitting procedure is a useful tool employed to reduce the noise and reconstruct the vegetation index time series. In the study conducted by Gumbricht (2016), the locally weighted scatterplot smoothing (LOWESS) method was utilized to effectively smooth the MODIS time series and model soil moisture dynamics. By applying this method, the resulting smoothed time series demonstrated increased robustness, enhancing the accuracy of identifying wetness phenology. A related study by Dai et al. (2022) further demonstrated the effectiveness of the LOWESS smoothing method in combination with the Random Forest algorithm's selection of three specific features: daily maximum temperature, daily cumulative radiation, and daily minimum temperature. Utilizing the LOWESS smoothing method resulted in minimized values for mean squared error, mean absolute difference, and mean absolute percentage error. Although the potential of LOWESS in detecting the date of phenological stages has been demonstrated in the above mentioned studies using optical remote sensing data, its application in time series analysis using SAR data has been relatively underexplored.

The determination of dates for important phenological stages in rice crops, such as transplanting and harvest, can be accomplished through the application of relative or absolute thresholds (Jenkins et al., 2002) or the identification of local extrema (Palacios-Orueta et al., 2012). Previous studies have successfully

utilized the identification of local extrema, specifically minimum and maximum values, to indicate various phenological stages in different crops. For instance, Palacios-Orueta et al. (2012) found that minima derived from fitted functions of MODIS time series data coincided with significant crop management dates during the growth period of cotton crops. Similarly, Schlund & Erasmi (2020) observed that the local maximum of Sentinel-1 time series data in VH polarization occurred after the mil ripeness stage, signifying the time of yellow ripeness or even harvest in wheat. In the context of Sentinel-1 SAR data, during the transplanting stage, when rice seedlings are transplanted and submerged in flooded fields, the dominant backscatter mechanism is the specular reflection on the water surface, resulting in minimal capture of backscatter coefficients by Sentinel-1 SAR (Clauss et al., 2018). Consequently, this minimum value can serve as a robust indicator of the transplanting date. Similarly, during the harvest stage, when rice plants reach maturity and are ready for harvesting, the backscatter coefficients are relatively higher compared to the initial crop establishment phase. Additionally, Mandal et al. (2018) noted that the backscatter coefficients were comparatively high after rice harvesting. Therefore, the peak of backscatter coefficients captured by a local maximum value can signify the harvest dates of rice crops. These local extrema act as reliable indicators of important stages in the rice growth cycle. Consequently, this study has thoroughly investigated the extraction of local extrema from Sentinel-1 time series by identifying local minimum and maximum values.

1.2. Problem statement

One of the United Nation's Sustainable Development Goals (SDGs) is to end hunger, achieve food security and improved nutrition and promote sustainable agriculture (United Nations, 2016). To realize this goal, it is necessary to ensure that sustainable crop production takes place, producing adequate food for all. Rice has been considered the most valuable crop in many countries and the staple food of the Philippines. Accurate estimation of transplanting and harvest dates can prevent asynchronous planting, which may be associated with a high disease incidence of rice crops, assist in the timely delivery of production inputs and guarantee farmers a reasonable market price for rice, promoting sustainable production. The above literature review reveals that researchers who investigated the rice crop season and phenological stages, such as germination, tillering, flowering and ripening, showed the potential of SAR data in detecting the dates of the phenological stages . However, most studies have focused on using SAR data on small-scale applications (at the commune level) and within the same season. The potential of Sentinel-1 data to detect both the transplanting and harvest dates in study areas with varying climate or rainfall distribution and at different seasons has not been examined.

The Philippines has a diverse climatology categorized into four climate types based on monthly rainfall distribution (Basconcillo et al., 2018). Hence, this study aims to explore the potential of multi-temporal Sentinel-1 SAR data for estimating the transplanting and harvest dates of rice crops at different seasons across regions with varying climates in the Philippines. The LOWESS function fitting procedure was employed in this research to extract local extrema, which were then compared with the data obtained from farmer surveys. The insights gained from this study can be valuable inputs for rice crop production simulations, enabling decision-makers to formulate policies that promote food security and social stability.

1.3. Objectives, research questions and hypotheses

The aim of this study is to assess the potential of multi-temporal Sentinel-1 SAR data in estimating the transplanting and harvest dates of rice crops across different seasons and provinces in the Philippines.

The specific objectives, research questions and hypotheses are:

a) To evaluate the performance of the LOWESS function fitting method in modelling the Sentinel-1 time series for rice crops.
    1. Research Question: To what extent does the LOWESS function fitting method effectively fit the original Sentinel-1 time series data for rice crops, ensuring noise reduction while preserving essential details?
    Hypothesis: The LOWESS function fitting method effectively reduces noise and preserves important details when fitting the original Sentinel-1 time series data for rice crops.

b) To determine the SAR metrics and local extrema that can be utilized to derive the transplanting and harvest dates of rice crops.
   1. Which SAR metrics and local extrema at various polarizations hold significance in the detection of transplanting and harvest dates of rice crops within the study area?
      Hypothesis: The utilization of specific SAR metrics and local extrema at various polarizations demonstrates a significant correlation with the accurate detection of transplanting and harvest dates of rice crops within the study area.

c) To assess the spatial and temporal transferability of the method used for estimating transplanting and harvest dates.
   1. Research Question: How does the method used for estimating transplanting and harvest dates demonstrate spatial and temporal transferability?
      Hypothesis: The method for estimating transplanting and harvest dates exhibit spatial and temporal transferability, demonstrating consistent accuracy across different spatial locations and seasons.

1.4. Conceptual diagram

The conceptual diagram (Figure 1.1) depicts the system boundary and the relationships between elements and processes within the system. It encompasses the entire Philippines as the main system. With rapid population growth, the country has an increasing demand for rice while agricultural land is diminishing due to conversion into residential or urban areas. The characteristics and conditions of crop fields are influenced by various factors, including crop types, planting methods, crop calendars, soil types, and water availability. Moreover, the weather and climate of the country significantly impact the crop fields. The farmers, supported by the Department of Agriculture, play a crucial role in managing the farms. The harvested crops, particularly rice, are then sold in the market, and consumers purchase food based on their dietary requirement

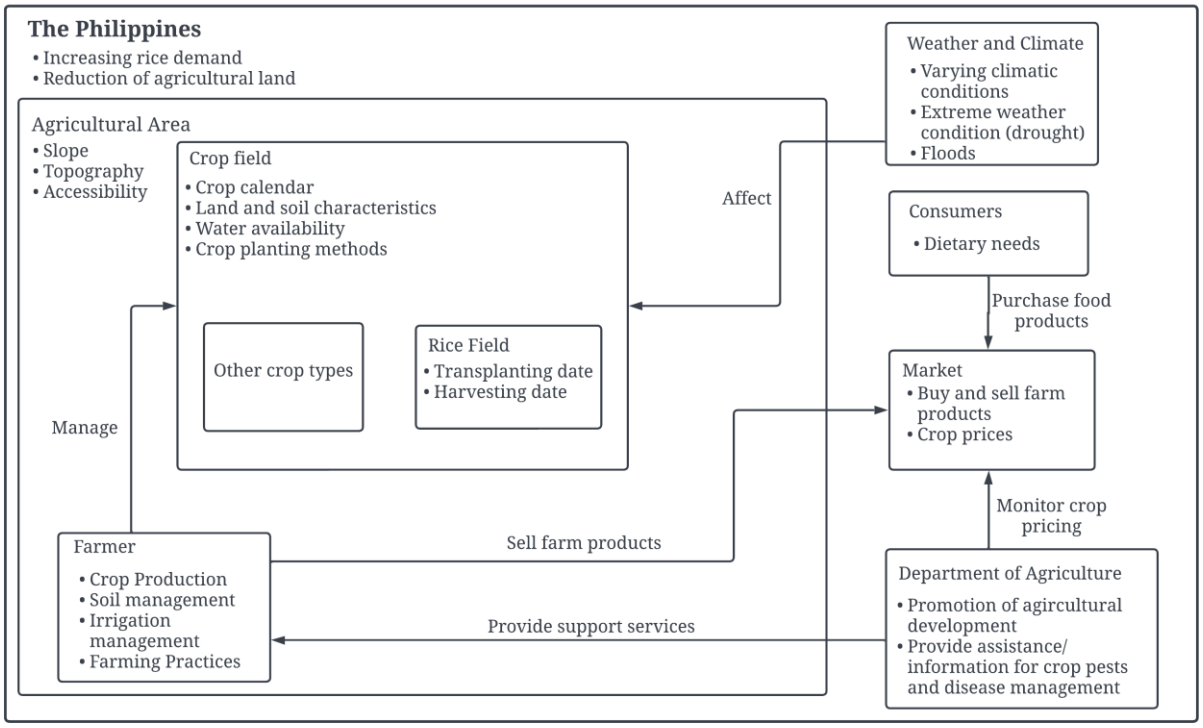

Figure 1.1 Conceptual diagram

2. STUDY AREA AND DATASETS

2.1. The Philippines

The study area encompasses the entire Philippine archipelago in Southeast Asia. It consists of 7,641 islands and is divided into three major island groups: Luzon, Visayas and Mindanao (FAO, 2022). The country spans between 4°23' north and 21°25' north latitudes, and 116° east and 127° east longitudes, with a total land area of 300,000 square kilometers (FAO, 2003). The Philippines is made up of 81 provinces, which are grouped into 17 regions. Its terrain is predominantly mountainous, with coastal lowlands. Agriculture plays a significant role in the Philippine economy due to the favorable soil conditions throughout the country, and many rural Filipinos depend on agricultural activities as their main source of income (Statista Research Department, 2021). For this study, three different provinces in the Philippines have been selected as the study area for estimating the transplanting and harvest dates of rice crops. These provinces are Cagayan (CGY) in Region 2, Leyte (LYT) in Region 8, and Agusan del Sur (ADS) in Region 13. Rice crops in the Philippines are typically cultivated during wet and dry seasons. In the country, the Department of Agriculture has implemented a crop calendar that defines the planting periods for rice based on two semesters. The dry season, referred to as semester 1, spans from September 16 to March 15. On the other hand, the wet season, known as semester 2, covers rice planting between March 16 and September 15 (Gutierrez et al., 2019). The Philippine climatology is characterized by its diversity, and it can be classified into four climate types based on the distribution of rainfall throughout the year (Figure 2.1).

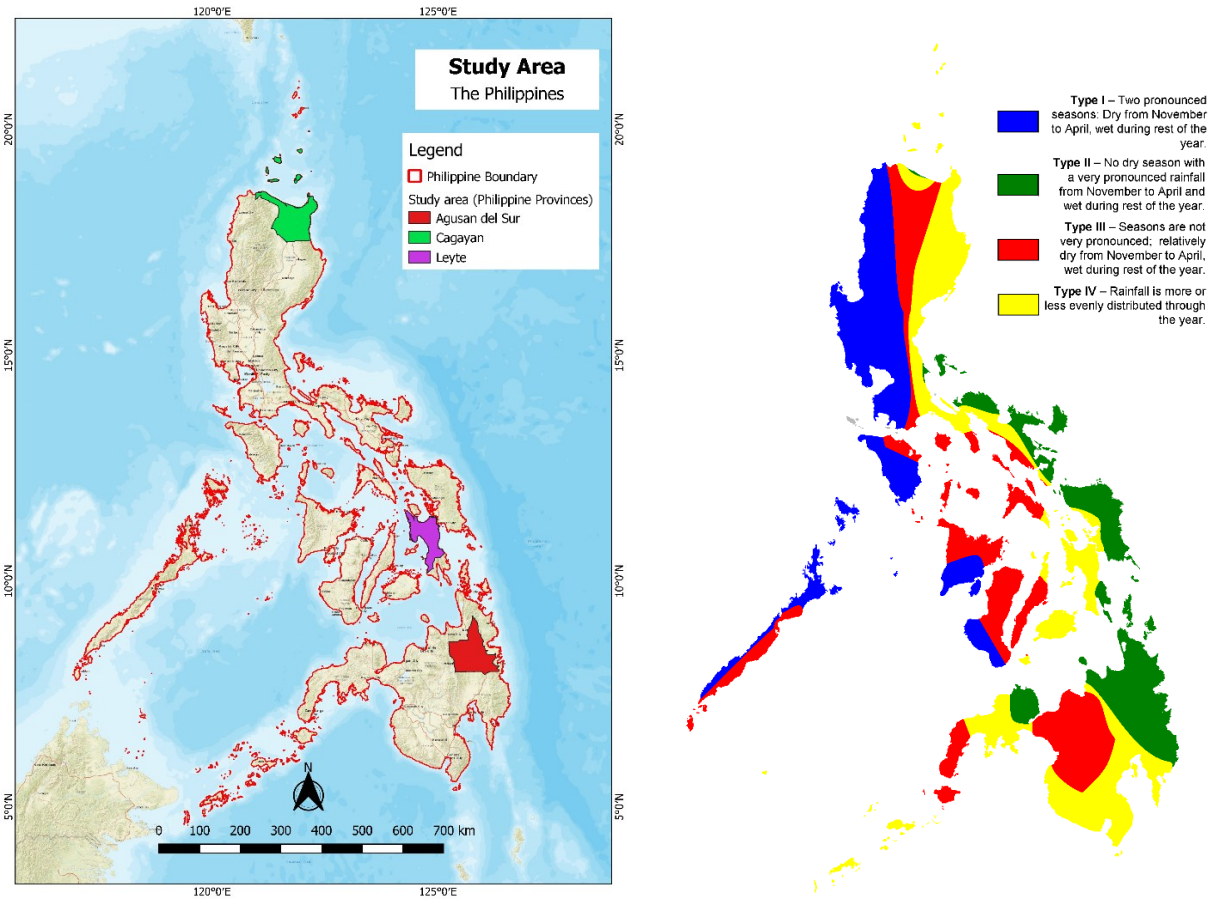

Figure 2.1 Location of the study area (Agusan (red), Cagayan (green) and Leyte (purple)) within the Philippines (left). Base map source: ESRI. and climate map of the Philippines (right). Source: MapSof.net

2.2. Farmers' interview and field survey data

This study utilized an existing dataset provided by the International Rice Research Institute (IRRI) as part of the Pest and Disease Risk Identification and Management (PRIME) project. Field data were collected from 99 rice fields in three provinces mentioned in the study area (19 fields in Agusan del Sur, 38 fields in Cagayan, and 42 fields in Leyte) were used for analysis. The data covered the period from 2017 to 2018 and included information gathered through interviews with farmers between February 17, 2019, and April 17, 2019.

The farmers' interviews captured data for two growing seasons: the wet and dry seasons in 2017-2018. These interviews gathered information about the rice fields, including crop types, crop establishment methods, crop calendars, land preparation, transplanting dates, flowering periods, and harvest dates. The specific focus of interest for validation purposes was the transplanting and harvest dates. However, the data has a midweek date as the event date instead of exact dates. To determine the appropriate duration of the time series to be analyzed, histograms (Figure 2.2 to Figure 2.7) were created for both transplanting and harvest dates. The dataset from the three provinces was utilized to test the methodology and evaluate the effectiveness of utilizing multi-temporal Sentinel-1 time series data in detecting transplanting and harvest dates of rice crops.

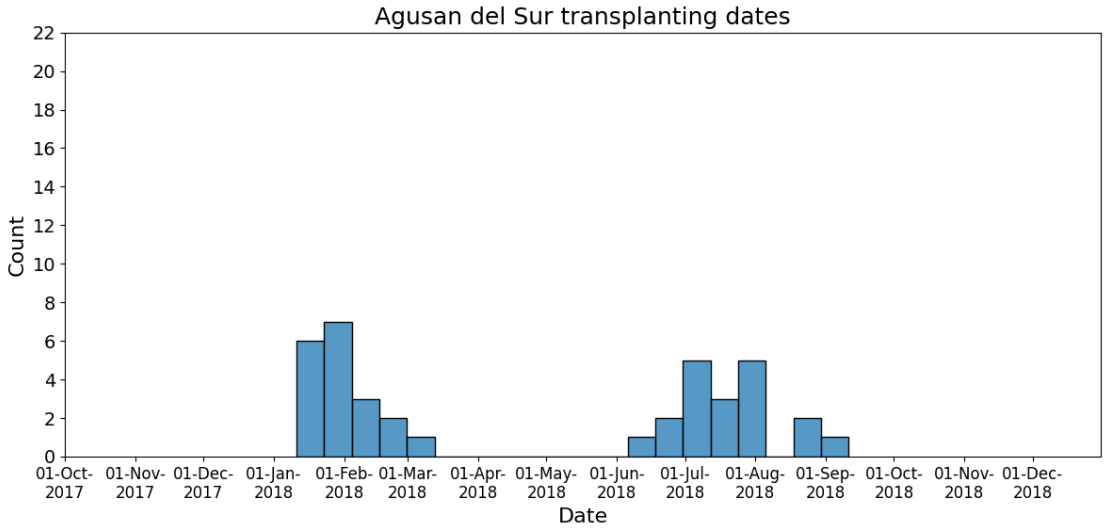

Figure 2.2 Distribution of transplanting dates for 19 rice fields in Agusan del Sur

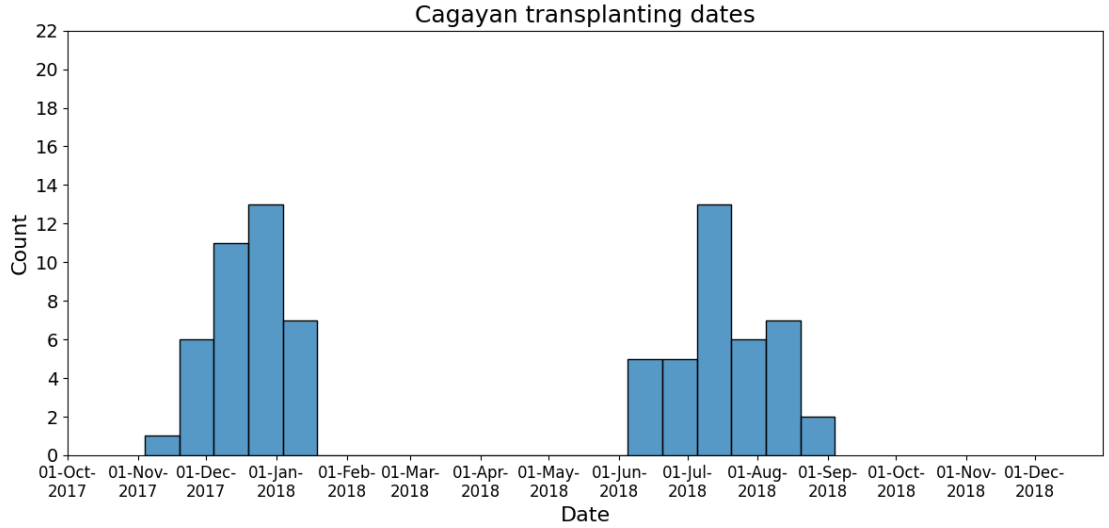

Figure 2.3 Distribution of transplanting dates for 38 rice fields in Cagayan

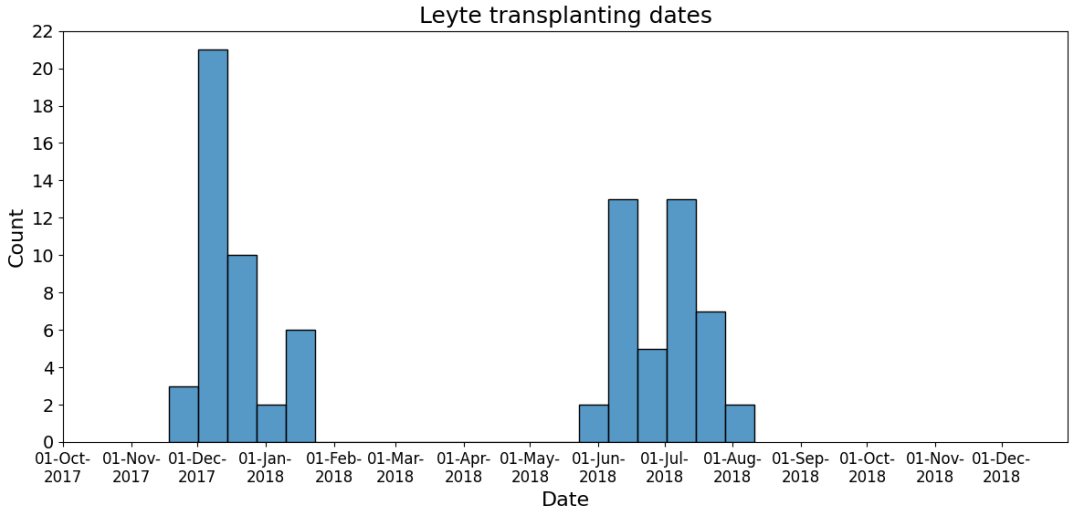

Figure 2.4 Distribution of transplanting dates for 42 rice fields in Leyte

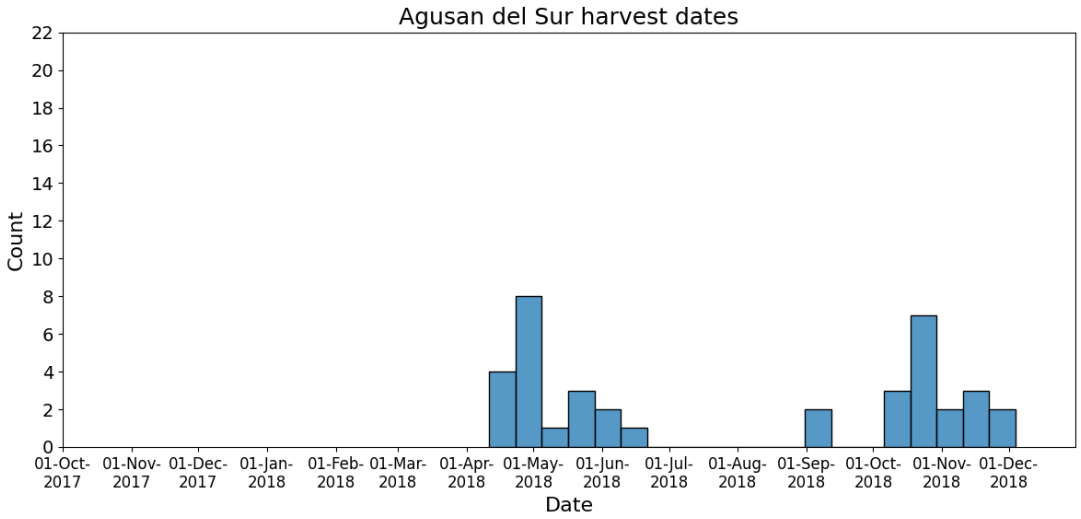

Figure 2.5 Distribution of harvest dates for 19 rice fields in Leyte

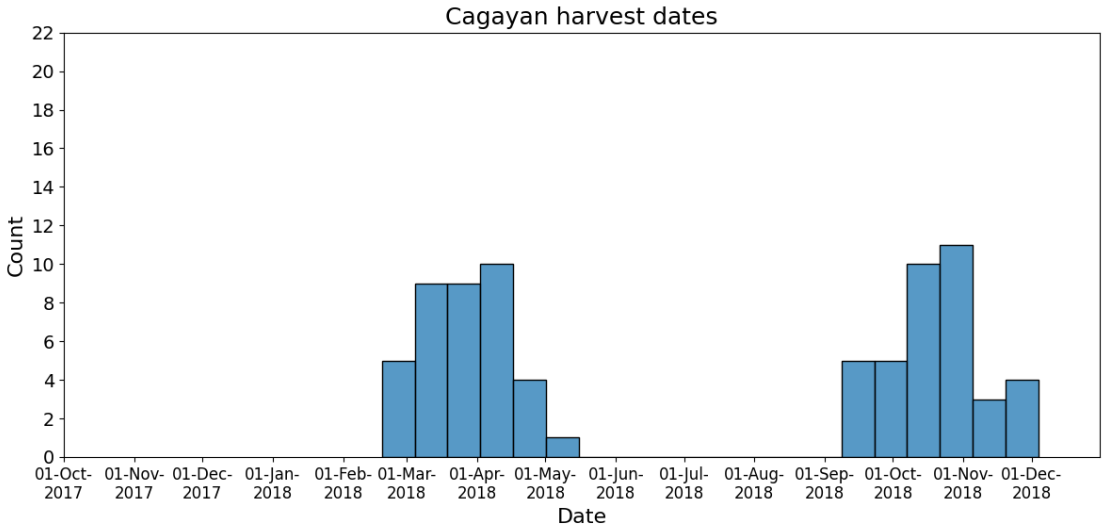

Figure 2.6 Distribution of harvest dates for 38 rice fields in Cagayan

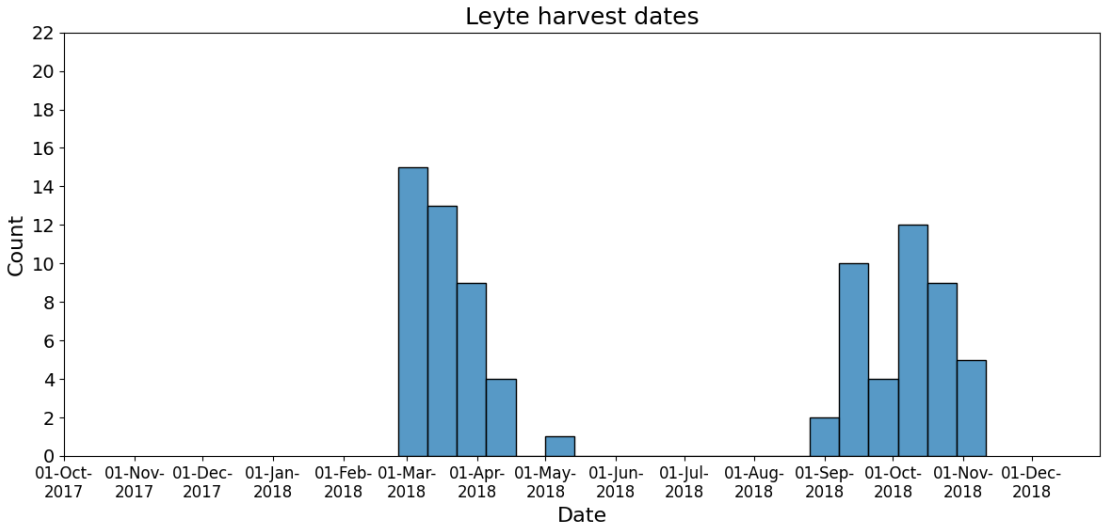

Figure 2.7 Distribution of harvest dates for 42 rice fields in Leyte

2.3. Sentinel-1 multi-temporal SAR data

The Sentinel-1 mission consists of two polar-orbiting satellites equipped with a C-band Synthetic Aperture Radar (SAR) imaging system. It was launched under the framework of the Copernicus programme by the European Space Agency (ESA) (Torres et al., 2017). Sentinel-1 SAR data from the ESA's Copernicus Hub was used in the study. The available Sentinel-1 products that are freely accessible include Level-1 data, which are provided in two formats: Single Look Complex (SLC) and Ground Range Detected (GRD) (Aulard-Macler, 2011). GRD products refer to SAR data, detected, multi-looked, and projected to ground range using an Earth ellipsoid model (Stasolla & Neyt, 2018). In addition, Sentinel-1 offers three common acquisition modes for GRD products: Interferometric Wide (IW) swath, Extra-Wide (EW) swath, and Stripmap (SM). This study specifically utilized the Sentinel-1 GRD SAR products with IW swath mode. This particular data has been extensively employed in various agricultural applications due to its suitability (Lasko et al., 2018; Torbick et al., 2017; Veloso et al., 2017). As Sentinel-1A data was already available, the Sentinel-1B data was pre-processed and extracted from the GEE (Google Earth Engine) platform. Table 2.1 presents the metadata of the dataset, providing additional information about its characteristics.

Table 2.1. Specifications of the Sentinel-1 data used in the study

Characteristic	**Description**
Satellite	Sentinel-1A and Sentinel-1B
Polarization	Dual polarimetry (VH, VV)
Repeat cycle	12 days per satellite
Orbit direction	Sun-synchronous (descending pass)
Band (central frequency)	C-band (5.405 GHz)
Azimuth and range resolution	22 m by 20 m
Pixel spacing	10 m by 10 m
Sensing mode	Interferometric Wide Swath (IW) mode
Incidence angle	30° to 46°

The backscatter coefficients extracted from Sentinel-1A and 1B are presented in Table 2.2 and Table 2.3, respectively. The dry and wet seasons were determined using the field survey data and the crop calendar established by the Department of Agriculture. The extracted data were integrated to generate a more frequent time series to enhance the temporal resolution. By combining the datasets of Sentinel-1A and 1B, the temporal resolution improved from 12 days to 6 days across the three provinces. However, there were

instances during the wet season when Sentinel-1B failed to capture backscatter information for certain periods. Specifically, in Agusan del Sur and Cagayan, the number of Sentinel-1B images was lower compared to Sentinel-1A. In other words, there were several occasions during the wet season when the Sentinel-1B backscatter coefficients were unavailable for these two provinces.

Table 2.2 Number of Sentinel-1A images used for extraction of backscatter coefficients

	Dry Season	Wet Season
Agusan del Sur	17	21
Cagayan	18	16
Leyte	17	18

Table 2.3 Number of Sentinel-1B images used for extraction of backscatter coefficients

	Dry Season	Wet Season
Agusan del Sur	18	16
Cagayan	18	10
Leyte	17	17

3. METHODOLOGY

3.1. Research methodology

Figure 3.1 depicts the flowchart of the methodology, comprising three distinct phases: Sentinel-1 SAR data processing, SAR metrics processing, and retrieval of transplanting and harvest dates. The first phase, Sentinel-1 SAR data processing, involves extracting Sentinel-1B time series data and integrating it with the existing Sentinel-1A time series data. IRRI was responsible for downloading and pre-processing Sentinel-1A data, while the NRS Department of ITC computed the mean backscatter for each field. The Sentinel-1B mean backscatter for each field was obtained through the GEE platform. The extracted mean backscatter coefficient in VV, VH, and the VH/VV polarizations were used as inputs for the time series analysis.

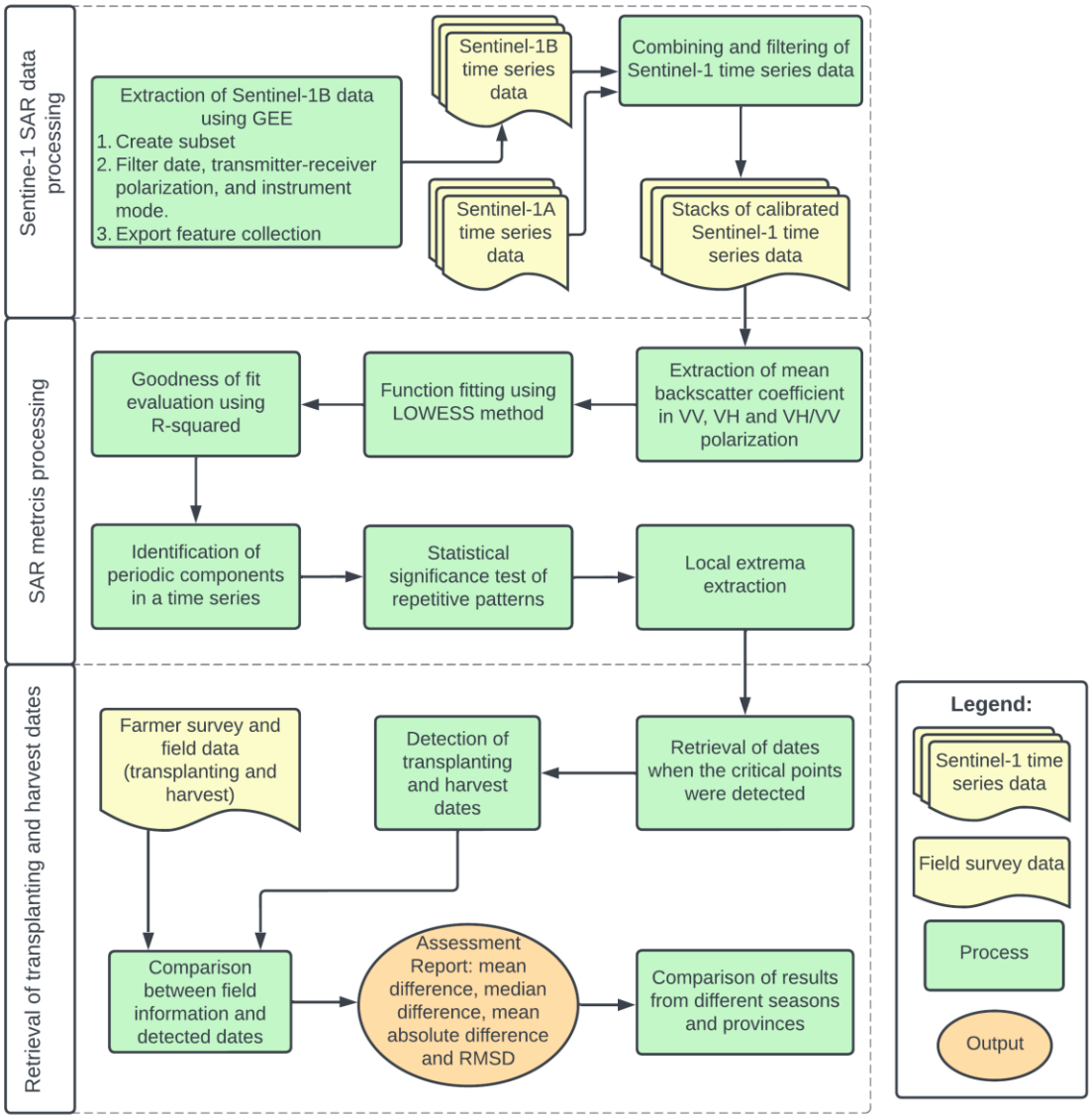

Figure 3.1 Methodology flowchart

The LOWESS function fitting method was employed in the second phase to smooth the time series data. The goodness of fit was evaluated by computing the coefficient of determination (R^2) between the original and LOWESS-smoothed time series curves. The number of periodic components or repetitive patterns in the time series was determined by employing periodogram analysis. To establish the statistical significance of the presence of repetitive patterns, the Breusch-Godfrey test was conducted. Subsequently, the SAR metrics and local extrema of the function fitted time series in VV, VH, and VH/VV were identified. The dates corresponding to the detection of local extrema were retrieved, and these dates were used to determine the transplanting and harvest dates of rice crops. Finally, the detected transplanting and harvest dates derived from the Sentinel-1 time series were compared to the information obtained from the field.

3.2. Sentinel-1 SAR data processing

The Sentinel-1A dataset provided by IRRI contains temporal backscatter coefficient values for each rice field. Due to the separate preprocessing of data from different seasons and overlapping dates between the end and start dates of seasons, the backscatter coefficients exhibited varying values in some instances. To address this issue, a mean value of the backscatter coefficient for each specific date was calculated and adopted as the representative value. This approach was implemented to ensure consistency and accuracy in cases where conflicting backscatter coefficient values were present.

The Sentinel-1B data was extracted using the GEE platform after receiving the Sentinel-1A data. The study area was defined by creating a subset or boundary using polygons representing the rice fields. The Sentinel-1B collection was filtered based on properties such as transmitter-receiver polarization, instrument mode, and date. The GEE platform automatically executed preprocessing steps to derive the backscatter coefficient for each pixel in the study area.

The Earth Engine 'COPERNICUS/S1_GRD' Sentinel-1 Image Collection showcases imagery obtained from Level-1 GRD scenes, which have been processed to represent the backscatter coefficient in decibels (dB) (Google Earth Engine Developers, 2022). The scattering behavior is influenced by various factors, including the physical characteristics of the terrain, such as the geometry of the terrain elements and their electromagnetic properties. To derive the backscatter coefficient for each pixel, Earth Engine employs a series of preprocessing steps, following the methodology implemented by the Sentinel-1 Toolbox. These steps include applying the orbit file, removal of GRD border noise, elimination of thermal noise, radiometric calibration, and terrain correction. These preprocessing techniques ensure the comparability and quality of the backscatter coefficient measurements obtained from the Sentinel-1 images in Earth Engine.

The backscatter coefficients per rice field were exported as tables. After obtaining the Sentinel-1A and B datasets, integration and filtering of the time series data were conducted. The ordering of the time series data was based on the acquisition dates. The resulting stacks of calibrated Sentinel-1 time series data were then utilized as inputs for extracting the mean backscatter coefficients in VV, VH and VH/VV polarizations.

3.3. LOWESS function fitting technique

To reconstruct the Sentinel-1 time-series curves and to make the data smooth, temporal filtering was performed through a LOWESS function fitting method, which is commonly employed in some remote sensing phenology analyses (Derkacheva et al., 2020; Gumbricht, 2016; Nilsson et al., 1997; Pouliot et al., 2008). The purpose of this smoothing process was to reveal underlying patterns and reduce noise while preserving important details. LOWESS is a non-parametric regression method that combines the benefits of scatterplot smoothing and local regression (Cleveland, 1979). It provides a flexible and adaptive method for modeling complicated data patterns by giving weights to neighboring data points.

3.3.1. Fraction parameter estimation using k-fold cross validation

In LOWESS, the fraction parameter plays a key role in determining the level of smoothing applied to the data (Cleveland, 1979). It determines the extent of the neighborhood or window used to calculate the local regression for each data point (Figure 3.2.). A larger fraction parameter incorporates more data points in the local regression calculation, resulting in a smoother fit (Derkacheva et al., 2020). It corresponds to a larger window size, which means a greater number of neighboring data points were considered when calculating the local regression. As a result, it yields a smoother curve or estimates of the underlying trend. Moreover, a larger fraction parameter assigns more weight to distant points, leading to a more global smoothing effect. Conversely, a smaller fraction parameter corresponds to a smaller window size, meaning fewer neighboring points were considered in the local regression calculation (Derkacheva et al., 2020). This results in a less smoothed curve or estimates that are more sensitive to local fluctuations. A smaller fraction parameter assigns more weight to nearby points, leading to a more localized or detailed smoothing effect.

The dominant optimal values for the fraction parameter in LOWESS smoothing were determined for each province, season and polarization through k-fold cross-validation. A standard choice for "k" is often 10, balancing computational efficiency and reliable model performance estimation (Fushiki, 2011). The dataset was divided into 10 equal-sized folds, allowing for iterative training and evaluation of the model. In each iteration, one fold served as the validation set, while the remaining folds were used for training (Wong & Yeh, 2020). This approach ensured a fair assessment of the model's performance across all folds. Mean squared error (MSE) was computed as a performance metric to evaluate different fraction parameter values (Wong & Yeh, 2020). Since the backscatter coefficients from Sentinel-1 were in decibels (dB), a conversion to the linear scale was performed using the formula:

$$\textbf{Linear value} = 10^{(dB/10)},$$

where dB represents the backscatter coefficient value in decibels. The MSE was then calculated based on the linear-scale data, enabling effective comparison and selection of the optimal fraction parameter for LOWESS smoothing. The fraction parameter with the lowest MSE was chosen as the optimal parameter. Afterward, the backscatter coefficients were transformed back to dB in order to apply LOWESS smoothing. The smoothing process utilized the dominant optimal fraction parameter identified for each season, province, and polarization. The iterative process of adjusting the fraction parameter and repeating k-fold cross-validation led to the identification of the value that achieved the highest model performance.

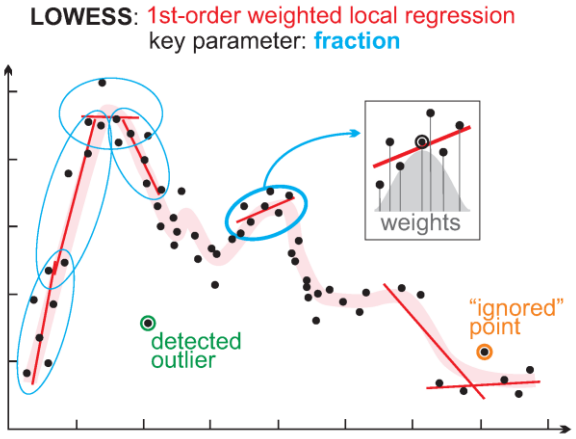

Figure 3.2 Principles of LOWESS. Black points are the source data; narrow red lines are the local regression solutions; the thick rose line is a final LOWESS solution. The gray area on the sub-panel represents a weight-defining function. Source: (Derkacheva et al., 2020)

3.3.2. Evaluation of the goodness of fit

To assess the effectiveness of the LOWESS temporal function fitting method in modelling the Sentinel-1 time series for rice crops, the evaluation of the goodness of fit between the original and LOWESS-smoothed time series curve involved calculating the coefficient of determination (R^2). R^2 quantifies the proportion of the original time series variance that is explained by the LOWESS-smoothed time series curve. A higher R^2 value indicates a better fit of the model or fitted function to the original data, suggesting a stronger relationship between the smoothed curve and the actual observations (Moore & McCabe, 1999). Conversely, a lower R^2 value indicates a poorer fit, indicating that the fitted function does not accurately capture the variability in the original time series (Moore & McCabe, 1999). The calculation of R^2 provides a valuable metric to assess the performance and suitability of the LOWESS smoothing approach for modelling the Sentinel-1 time series of rice crops, providing insights into the accuracy and reliability of the obtained smoothed curves.

3.4. Periodogram analysis and statistical significance test

Periodogram analysis, which identifies periodic patterns in a time series, was employed to determine the presence and number of repeated patterns in the data (Palacios-Orueta et al., 2012). By examining the periodogram, the general pattern of the fitted function can be understood, and the number of local extrema can be identified. This analysis helps to determine whether there is a single or double cycle during the growing period in the LOWESS-smoothed time series. A statistical significance test called the Breusch-Godfrey (BG) test was conducted to verify the presence of these repetitive patterns. BG test is widely used to examine autocorrelation in errors (Breusch, 1978; Godfrey, 1978). It is a popular choice among practitioners due to its ease of application and applicability in the presence of lagged dependent variables, allowing for a comprehensive assessment of serial correlation in errors (Edgerton & Shukur, 2007; Mahan et al., 2015). The purpose of the BG test in this context was to determine whether the observed data variations deviate significantly from white noise or random fluctuations that a regression model cannot explain. According to Fuller (1996), the confirmation that the backscatter coefficients represent white noise suggests the absence of any periodic component. In other words, if the backscatter coefficients exhibit characteristics of white noise, it implies that there are no discernible repetitive patterns or periodicity present in the data.

3.5. Retrieval of transplanting and harvest dates

The LOWESS smoothing process generated a smoothed time series curve, capturing the underlying patterns and reducing noise in the Sentinel-1 data for rice crops. From this smoothed curve, various SAR metrics and local extrema were extracted, encompassing the local minima and local maxima of the different Sentinel-1 polarizations. Identifying and analyzing these local extrema are essential for assessing the overall shape and behavior of the function-fitted time series. The presence and count of local maxima and minima provide insights into the cyclical nature and growth patterns exhibited by the time series (Palacios-Orueta et al., 2012). Specifically, the presence of one local maximum or minimum may indicate that the function-fitted time series has the shape of a single cycle through a growing period. Point x was identified as the local maxima if $f(x) \geq f(x_0)$, while point x was defined as a local minima if $(x) \leq f(x_0)$, where x_0 is the point next to x (Schlund & Erasmi, 2020).

To estimate the transplanting and harvest dates of rice crops, the identified local extrema in VV, VH, and VH/VV polarizations were associated with specific dates. The dates associated with the detected local minima were indicative of the transplanting date, as the rice seedlings are transplanted and submerged in flooded fields, resulting in low backscatter coefficients due to specular reflections on the water surface. Conversely, the dates associated with the detected local maxima were associated with the harvest date, as higher backscatter coefficients are observed due to volume scattering. By leveraging these associations, accurate estimates of rice crop transplanting and harvest dates can be obtained.

3.6. Field information and detected dates comparison

The reported field information on transplanting and harvest dates from farmers in three provinces was compared to the dates of the local extrema identified in the LOWESS-smoothed time series curve of VV, VH, and VH/VV polarizations. To assess the temporal disparity between the farmer-reported and detected transplanting and harvest dates during the dry season, a histogram was generated. This visualization allowed for the identification of potential outliers. The presence of outliers in the results could be attributed to factors such as inaccuracies in the reported dates by farmers or the presence of noisy time series data, which can hinder the accurate estimation of transplanting and harvest dates. To account for the potential influence of outliers, a robust measure known as the median absolute deviation (MAD) was employed. The MAD is a scale measure based on the median of the absolute differences between each data point and the median of the dataset (Howell, 2005). In univariate statistics, the MAD is widely regarded as a reliable measure of dispersion/scale, particularly when dealing with outliers (Elamir, 2012). Choosing an appropriate threshold for outlier detection is essential to ensure that the criteria used are not based on randomly selecting degrees of freedom. In this study, the median plus or minus 2.5 times the MAD was employed, where a threshold value of 2.5 was deemed a reasonable choice (Leys et al., 2013). This approach helped mitigate the impact of outliers and enhance the accuracy of estimating transplanting and harvest dates for rice crops.

The effectiveness of the method used for detecting transplanting and harvest dates was assessed by reporting an assessment result. Variations may indicate that the farmer-reported dates may occur before or after local extrema. Mean differences, median differences, root mean squared differences (RMSD), and mean absolute differences were calculated to quantify the differences between the farmer-reported and detected dates. These are commonly used measures to evaluate the performance of methods (Andrade, 2020; Miralles et al., 2010). The assessment results of the three provinces were compared to evaluate the applicability of the method in areas with different climatic conditions. The time series analysis was implemented using Python IDLE.

4. RESULTS

4.1. LOWESS function fitting technique

4.1.1. Fraction parameter estimation using k-fold cross validation

The dominant optimal fraction parameters used for smoothing Sentinel-1 time series curve for each province, considering the season and polarization are presented in Table 4.1. As can be seen from the table, for the VH polarization combination across all images, a fraction parameter of 0.3 was the most optimal. However, for VV and VH/VV polarizations, the dominant optimal fraction parameters varies depending on the season and study area. Specifically, during the dry season, Agusan del Sur and Leyte predominantly have a fraction parameter of 0.3, while Cagayan has a dominant value of 0.5. In contrast, during the wet season, Agusan del Sur and Cagayan have a predominant fraction parameter of 0.5, while Leyte has a dominant value of 0.3.

Table 4.1 Optimal fraction parameter per season per province and per polarization

	Fraction Parameter	
Agusan del Sur	Dry season	Wet season
VH	0.3	0.3
VV	0.3	0.5
VH/VV	0.3	0.5
Cagayan	Dry season	Wet season
VH	0.3	0.3
VV	0.5	0.5
VH/VV	0.5	0.5
Leyte	Dry season	Wet season
VH	0.3	0.3
VV	0.3	0.5
VH/VV	0.5	0.3

4.1.2. Evaluation of the goodness of fit

The evaluation of the goodness of fit varied depending on the distribution of data, with low R^2 values observed for time series data characterized by pronounced fluctuations and variability. The variations in backscatter coefficients are evident in the Sentinel-1 original and LOWESS-smoothed time series curves for a selected field in Leyte as shown in Figure 4.1, Figure 4.2 and Figure 4.3. Employing the fitted time series curve, the noise and fluctuations in the time series have been minimized, revealing a discernable pattern. For the selected field in Leyte, a consistent optimal fraction parameter of 0.3 was used for all polarizations. The results show that VH and VV polarizations have higher R^2 values of 0.61 and 0.63, respectively, compared to the VH/VV polarization with an R^2 value of 0.17.

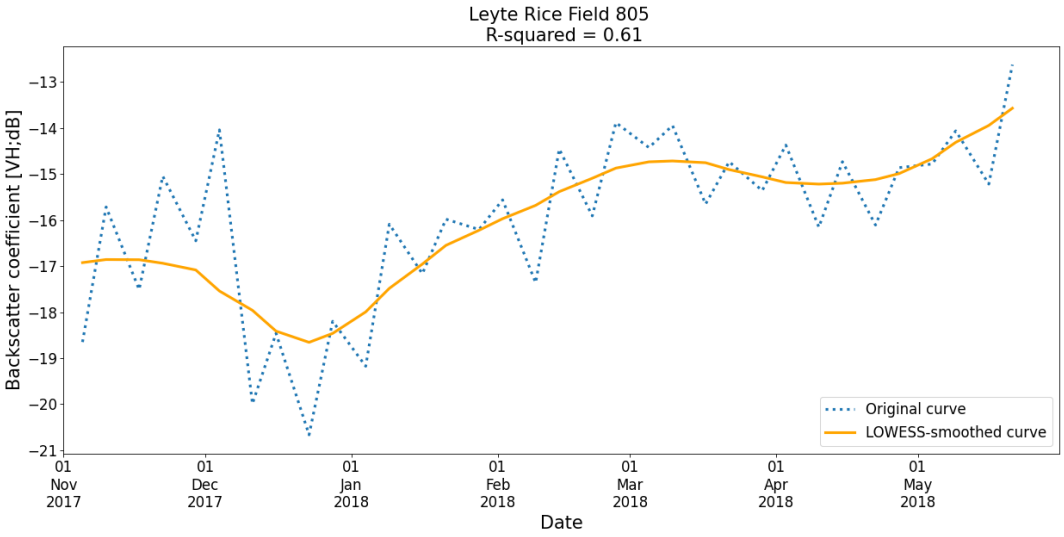

Figure 4.1 Sentinel-1 original vs fitted time series curves of field 805 in Leyte (VH polarization)

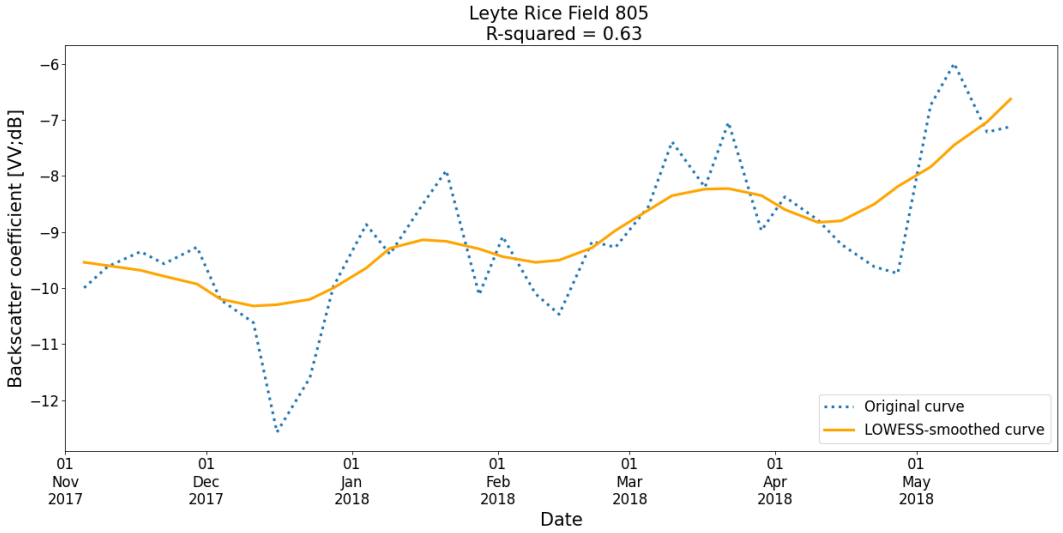

Figure 4.2 Sentinel-1 original vs fitted time series curves of field 805 in Leyte (VV polarization)

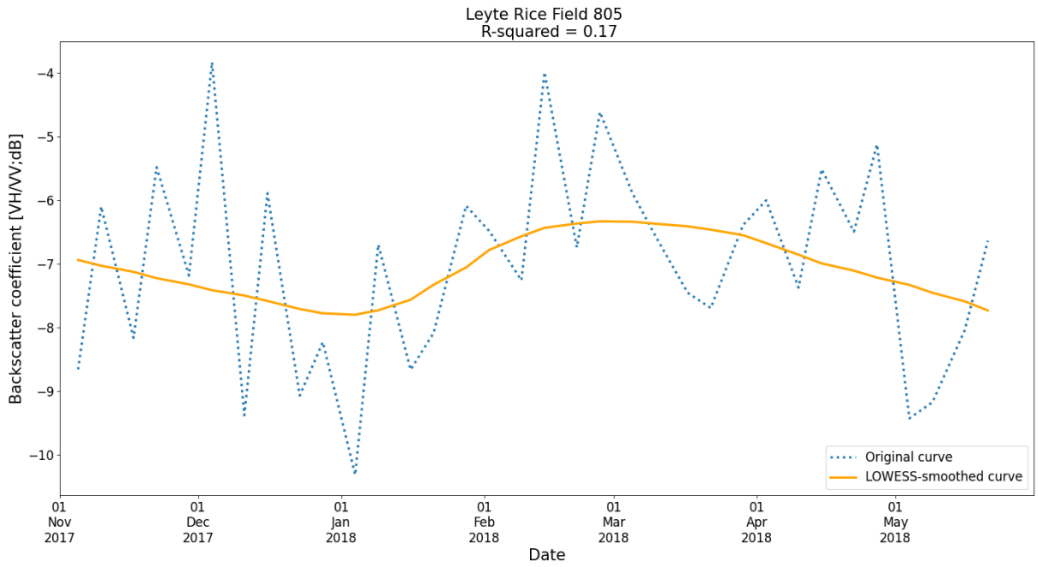

Figure 4.3 Sentinel-1 original vs fitted time series curves of field 805 in Leyte (VH/VV polarization)

Each province consists of six boxplots representing the R^2 values between the Sentinel-1 original and LOWESS-smoothed time series curves for three different polarizations in two seasons (Figure 4.4, Figure 4.5 and Figure 4.6). The analysis indicates that, in general, the VV data during the wet season exhibits the lowest R^2 values (median $R^2 < 0.4$), indicating weaker linearrelationships between the original and LOWESS-smoothed time series curves. Figure 4.7 shows the linear relationship between the original and LOWESS-smoothed time series curves of a selected rice field in Leyte for VV polarization during the wet season. Additionally, Agusan del Sur and Leyte provinces demonstrate a wider dispersion of R^2 values for VV polarization during the wet season compared to Cagayan province. On the other hand, the VH data predominantly showcases the highest R^2 values (median $R^2 > 0.59$), among the three polarizations. This implies stronger linear relationships between the original and LOWESS-smoothed time series curves in VH polarization across all three provinces. Figure 4.8 shows the linear relationship between the original and LOWESS-smoothed time series curves of a selected rice field in Leyte for VH polarization during the dry season.

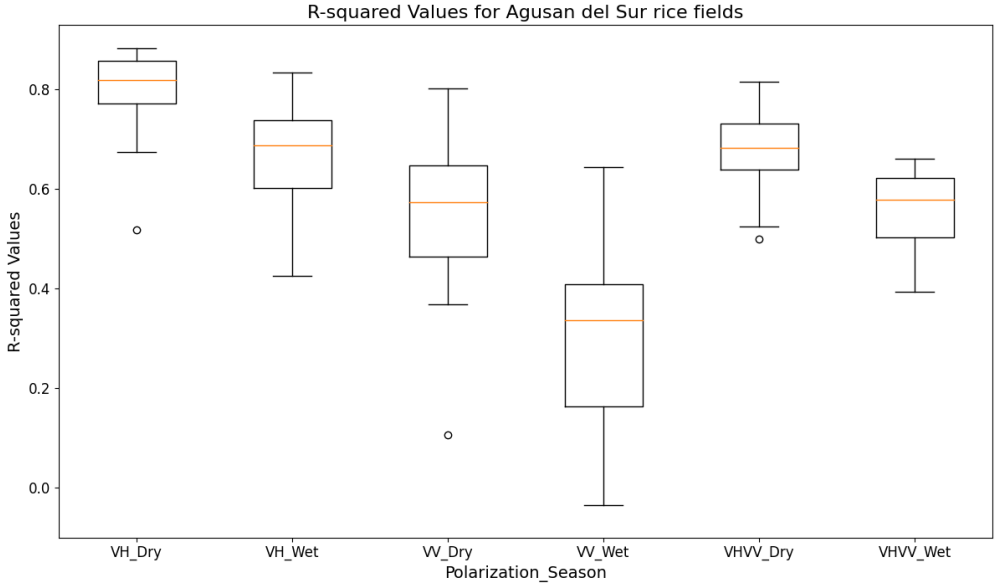

Figure 4.4 R^2 values between the original and fitted time series curve for Agusan del Sur rice fields

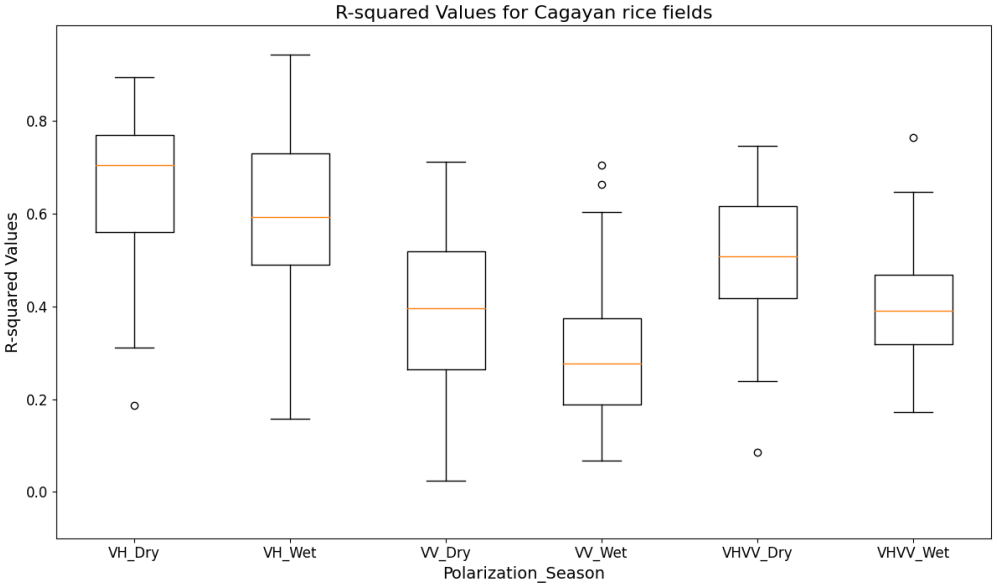

Figure 4.5 R^2 values between the original and fitted time series curve for Cagayan rice fields

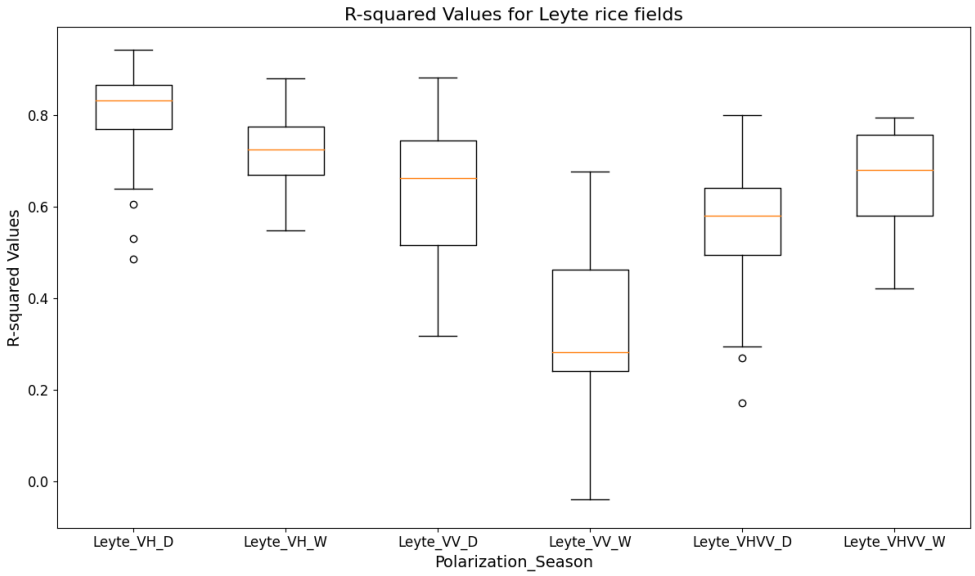

Figure 4.6 R^2 values between the original and fitted time series curve for Leyte rice fields

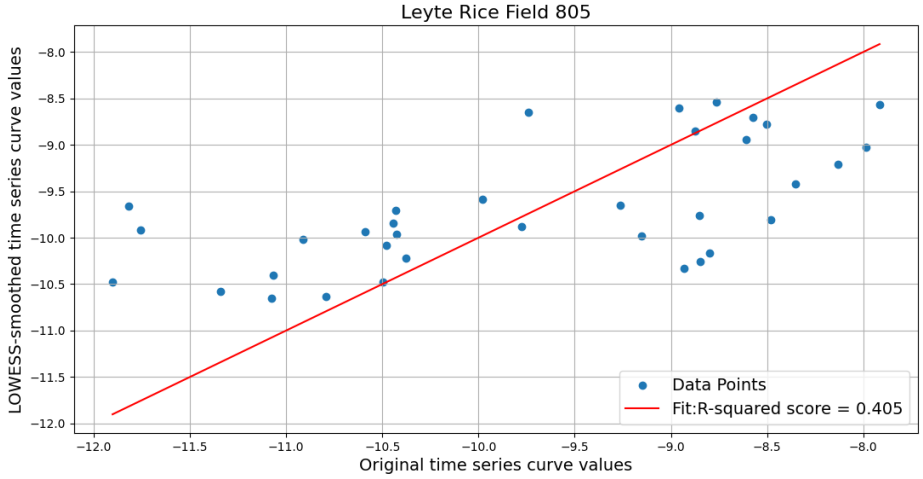

Figure 4.7 Relationship between the original and LOWESS-smoothed time series curves of field 805 in Leyte for VV polarization during the wet season

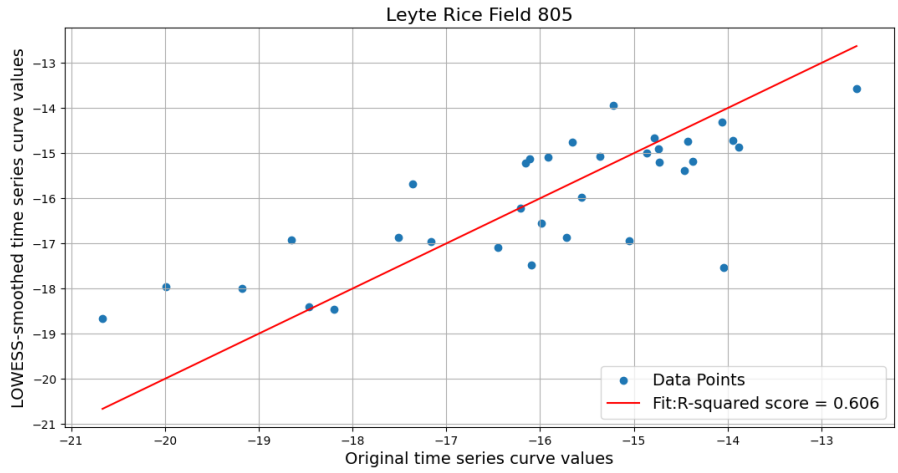

Figure 4.8 Relationship between the original and LOWESS-smoothed time series curves of field 805 in Leyte for VH polarization during the dry season

4.2. Periodogram analysis and statistical significance test

The periodogram analysis reveals that the majority of the time series data in all provinces exhibit a predominant single period or cycle, while a smaller number displays two or three periods or cycles (Table 4.2). These findings indicate that the time series curves consistently demonstrate the presence of a unique cycle, representing the period from transplanting to harvest of rice crops across all polarizations and provinces, regardless of the season. The existence of a single cycle suggests distinct patterns and fluctuations in rice growth and development.

Table 4.2 Periodic components of the time series in different polarizations

	Dominant Period	
ADS	Dry season (Dec 2017 – Jun 2018)	Wet season (May – Dec 2018)
VH	19 (single)	14(single), 5 (double)
VV	14 (single), 2 (double), 3 (triple)	14 (single), 5 (double)
VH/VV	17 (single), 2 (double)	16 (single), 3 (double)
Cagayan	Dry season (Nov 2017 – May 2018)	Wet season (Jun – Dec 2018)
VH	27 (single), 11 (double)	29 (single), 9 (double)
VV	33 (single), 5 (double)	27 (single), 11 (double)
VH/VV	28 (single), 10 (double)	24 (single), 14 (double)
Leyte	Dry season (Nov 2017 – May 2018)	Wet season (May – Nov 2018)
VH	42 (single)	39 (single), 2 (double), 1 (triple)
VV	36 (single), 6 (double)	36 (single), 6 (double),
VH/VV	41 (single), 1 (double)	33 (single), 9 (double)

The results of the Breusch-Godfrey white noise test offer further insights into the nature of the data (Table 4.3). In the Breusch-Godfrey test, the majority of the data yield statistically significant p-values at a significance level of 0.05. Consequently, the null hypothesis, which assumes the absence of any systematic patterns, autocorrelation and periodic components in the time series data, is rejected. These significant results indicate that most of the analyzed data exhibit non-white noise characteristics, suggesting the presence of discernable patterns rather than randomness. Additionally, these results substantiate the outcomes of the periodogram analysis, which identifies the number of periodic components in the time series. The results from the different analyses, such as the periodogram analysis and Breusch-Godfrey white noise test, support each other and indicate consistent patterns and connections in the data.

Table 4.3 Breusch-Godfrey white noise test results

	White noise test result	
ADS	Dry season (Dec 2017 – Jun 2018)	Wet season (May – Dec 2018)
VH	All non-white noise	All non-white noise
VV	All non-white noise	All non-white noise
VH/VV	All non-white noise	All non-white noise
Cagayan	Dry season (Nov 2017 – May 2018)	Wet season (Jun – Dec 2018)
VH	All non-white noise	36 non-white noise, 2 white noise
VV	All non-white noise	All non-white noise
VH/VV	All non-white noise	All non-white noise
Leyte	Dry season (Nov 2017 – May 2018)	Wet season (May – Nov 2018)
VH	41 non-white noise, 1 white noise	All non-white noise
VV	37 non-white noise, 5 white noise	All non-white noise
VH/VV	All non-white noise	All non-white noise

4.3. Retrieval of transplanting and harvest dates

The fitted time series curves exhibit a distinctive temporal pattern, with decreasing backscatter coefficients approaching the transplanting period and increasing backscatter coefficients approaching the harvest period. This pattern enables the identification of transplanting and harvest dates based on the local minimum and maximum values in the time series curves. For instance, in a selected rice field in Leyte during the dry season, the VH, VV and VH/VV polarizations indicate transplanting dates of December 23, 2017, December 11, 2017, and January 4, 2018, respectively, while the farmer reported a transplanting date of December 11, 2017 (Figure 4.9, Figure 4.10 and Figure 4.11). The first local minimum in all three polarizations closely aligns with the farmer-reported transplanting date, with VV polarization matching exactly. For harvest dates in the same rice field and season, VH, VV and VH/VV polarizations indicate harvest dates of March 10, 2018, March 22, 2018, and February 26, 2018, respectively, while the farmer reported a harvest date of March 11, 2018 (Figure 4.9, Figure 4.10 and Figure 4.11). Harvest dates are estimated using the local maximum following the local minimum in VH and VH/VV polarizations and the second local maximum after the first local minimum in VV polarization, except when only one local maximum existed, in which case that date is used.

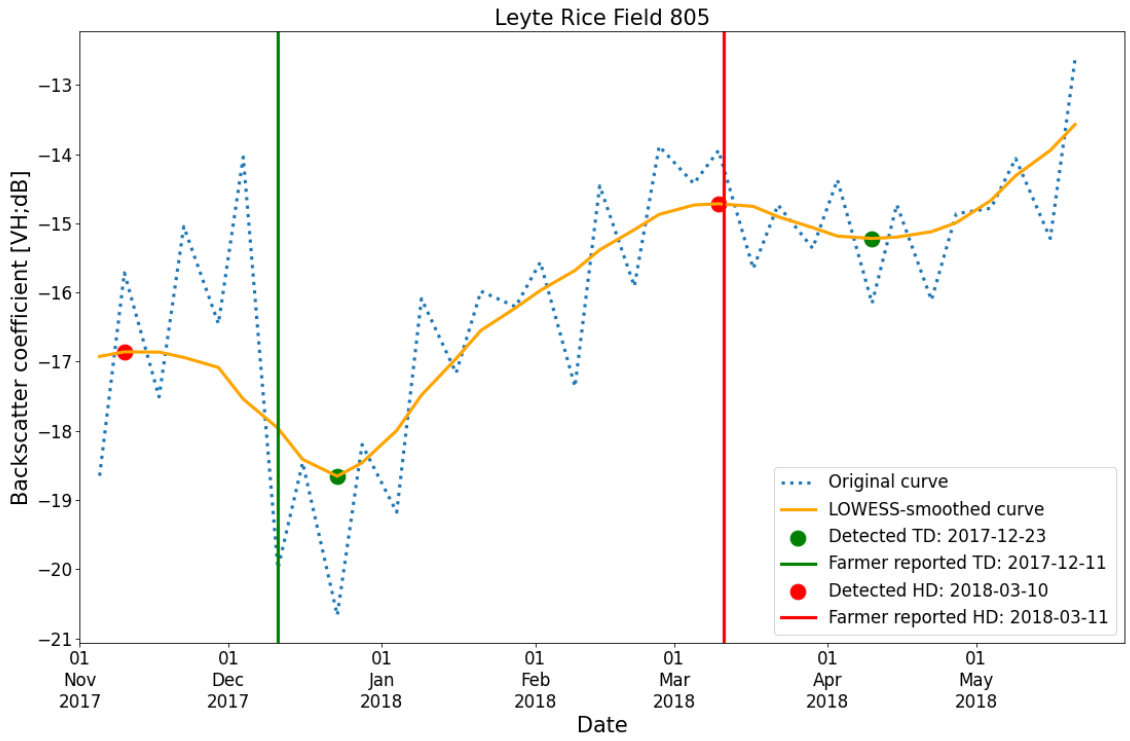

Figure 4.9 SAR VH backscatter coefficients and LOWESS-smoothed time series curve with farmer-reported and detected dates for field 805 in Leyte during the dry season

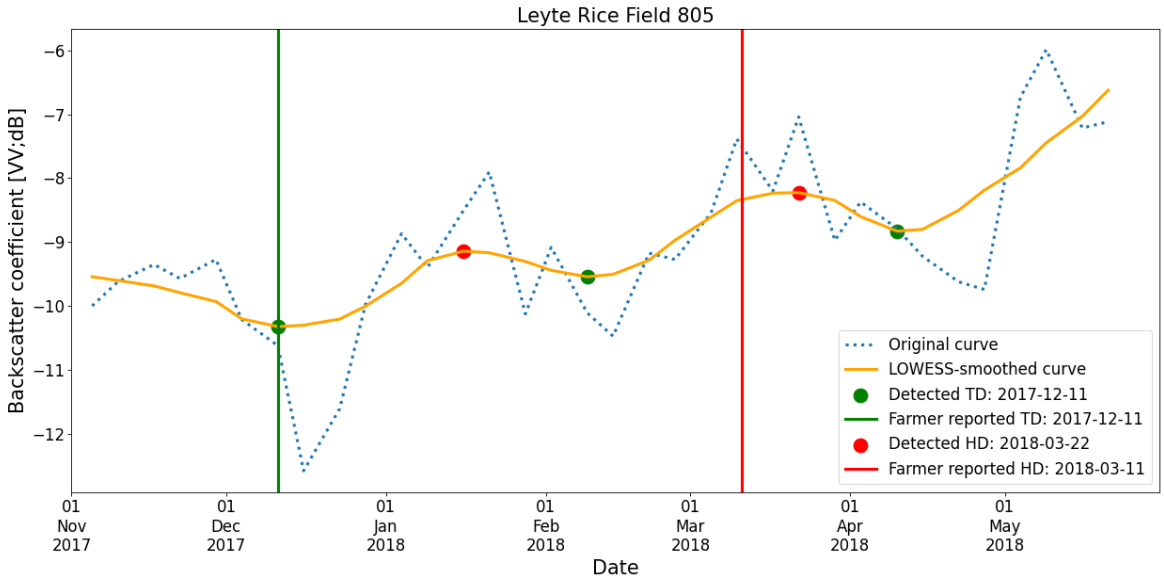

Figure 4.10 SAR VV backscatter coefficients and LOWESS-smoothed time series curve with farmer-reported and detected dates for field 805 in Leyte during the dry season

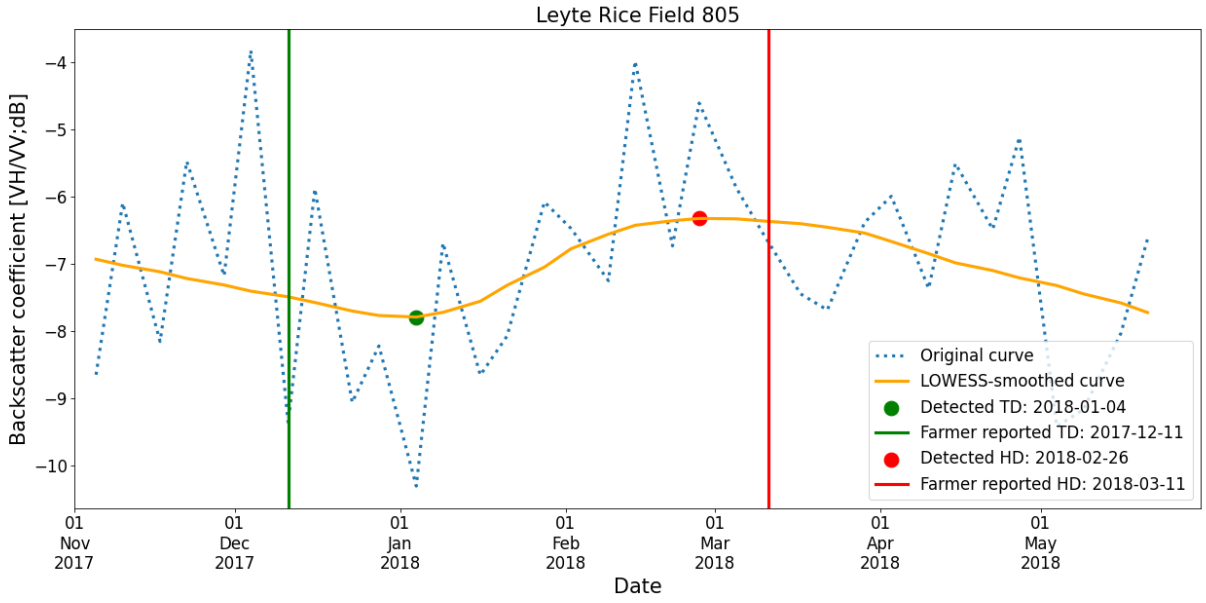

Figure 4.11 SAR VH/VV backscatter coefficients and LOWESS-smoothed time series curve with farmer-reported and detected dates for field 805 in Leyte during the dry season

4.4. Field information and detected dates comparison

The histograms in Figure 4.12 to Figure 4.17 demonstrate the temporal difference (in days) between the farmer-reported and detected transplanting and harvest dates during the dry season. It can be observed that there are some outliers in the data. Hence, a median absolute deviation (MAD) was employed to address this issue and remove the potential outliers from the data.

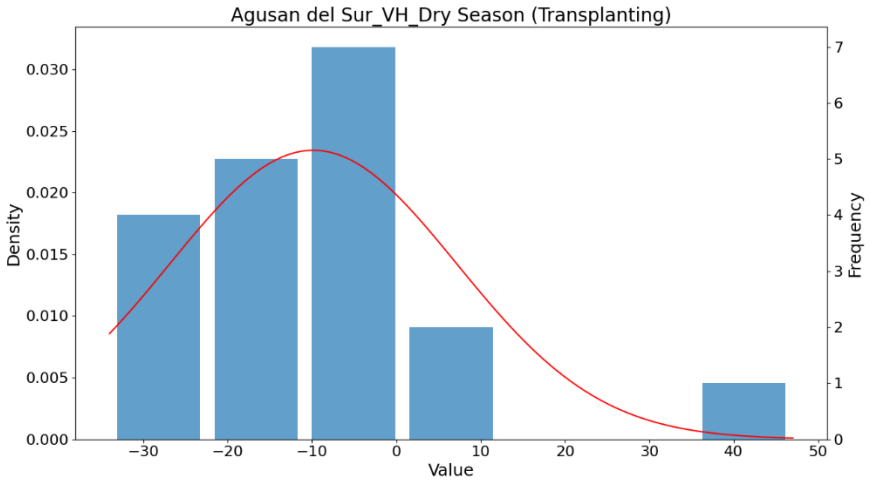

Figure 4.12 Histogram of the difference in days between the farmer-reported and detected transplanting date in Agusan del Sur for VH polarization during the dry season

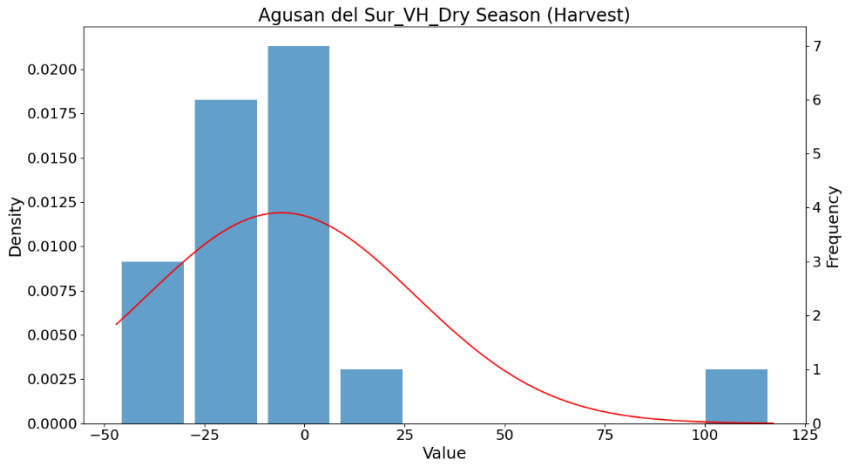

Figure 4.13 Histogram of the difference in days between the farmer-reported and detected harvest date in Agusan del Sur for VH polarization during the dry season

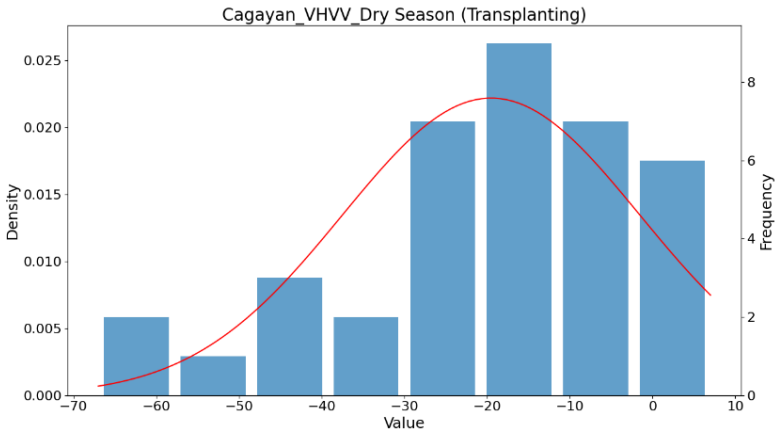

Figure 4.14 Histogram of the difference in days between the farmer-reported and detected transplanting date in Cagayan for VH/VV polarization during the dry season

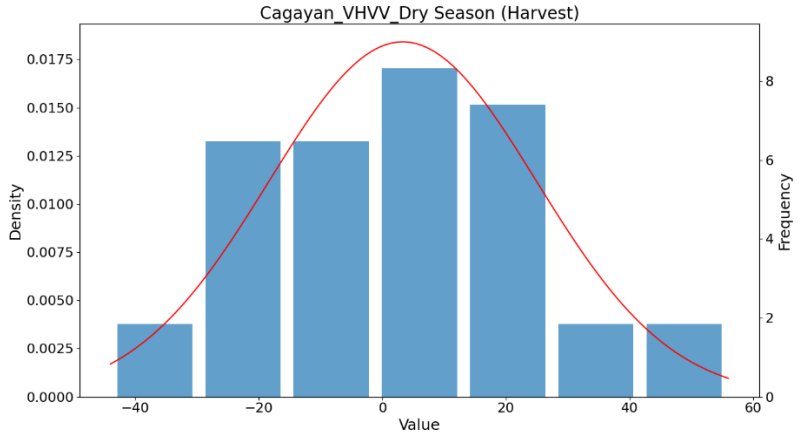

Figure 4.15 Histogram of the difference in days between the farmer-reported and detected harvest date in Cagayan for VH/VV polarization during the dry season

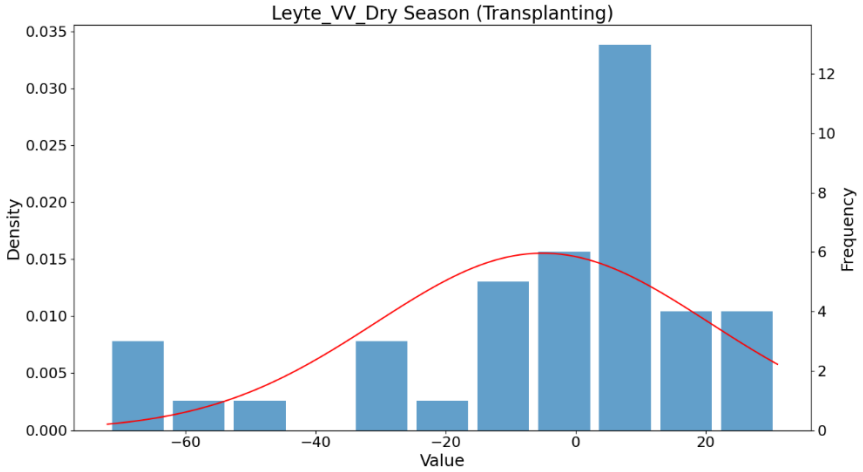

Figure 4.16 Histogram of the difference in days between the farmer-reported and detected transplanting date in Leyte for VV polarization during the dry season

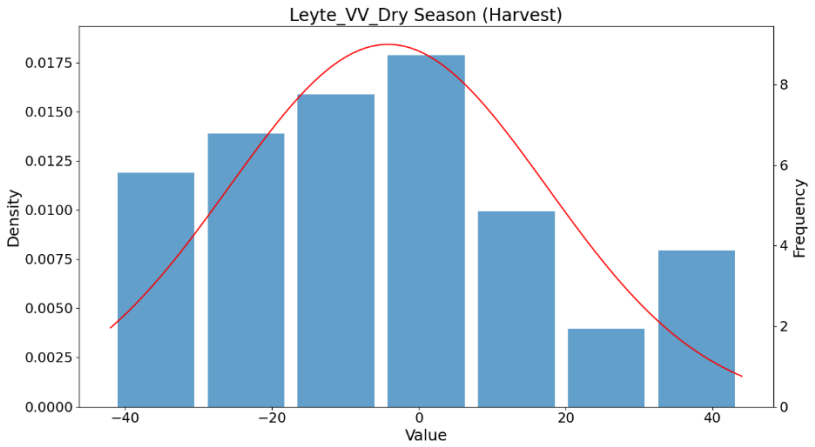

Figure 4.17 Histogram of the difference in days between the farmer-reported and detected harvest date in Leyte for VV polarization during the dry season

After applying the MAD method for outlier removal, a generated assessment report on comparing field information and detected dates is presented in Appendix 2. Comparison between field information and detected dates). However, it should be noted that some rice fields are excluded from the final assessment. These fields are excluded either because they do not exhibit local minimum or local maximum characteristics, or because they are considered outliers during the MAD outlier removal process (Table 4.4).

Table 4.4 Number of rice fields excluded in the final assessment

		Absence of local min.	Local min considered as outlier	Absence of local max.	Local max considered as outlier
Agusan del Sur (dry season)	VH	0	4	1	2
	VV	0	3	0	3
	VHVV	0	0	1	0
Agusan del Sur (wet season)	VH	0	2	0	8
	VV	0	3	2	5
	VH/VV	1	5	2	4
Cagayan (dry season)	VH	0	5	0	3
	VV	17	2	16	2
	VH/VV	1	7	1	4
Cagayan (wet season)	VH	0	4	0	6
	VV	3	7	2	8
	VHVV	3	3	1	6
Leyte (dry season)	VH	2	4	6	5
	VV	5	4	3	5
	VH/VV	2	3	21	1
Leyte (wet season)	VH	2	1	3	9
	VV	3	5	16	3
	VH/VV	2	7	2	1

For the final assessment, the results are illustrated in boxplots (Figure 4.18 to Figure 4.23) illustrating the temporal difference between the farmer-reported and detected transplanting and harvest dates for all polarizations in all three provinces during the wet and dry seasons. These boxplots provide insights into the distribution and variability of the results. Notably, any outliers have been eliminated from the figures.

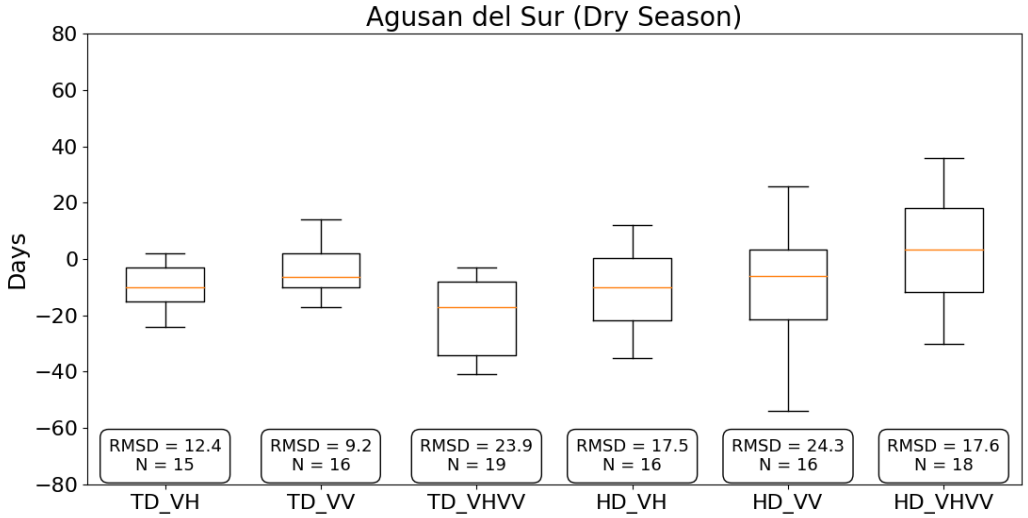

Figure 4.18 Boxplots of the temporal difference between the farmer-reported and detected transplanting and harvest dates in Agusan del Sur during the dry season

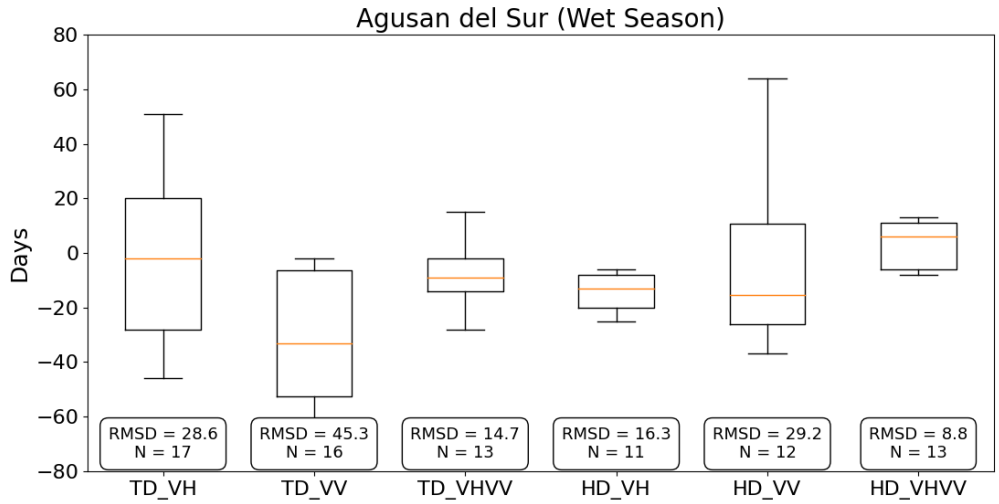

Figure 4.19 Boxplots of the temporal difference between the farmer-reported and detected transplanting and harvest dates in Agusan del Sur during the wet season

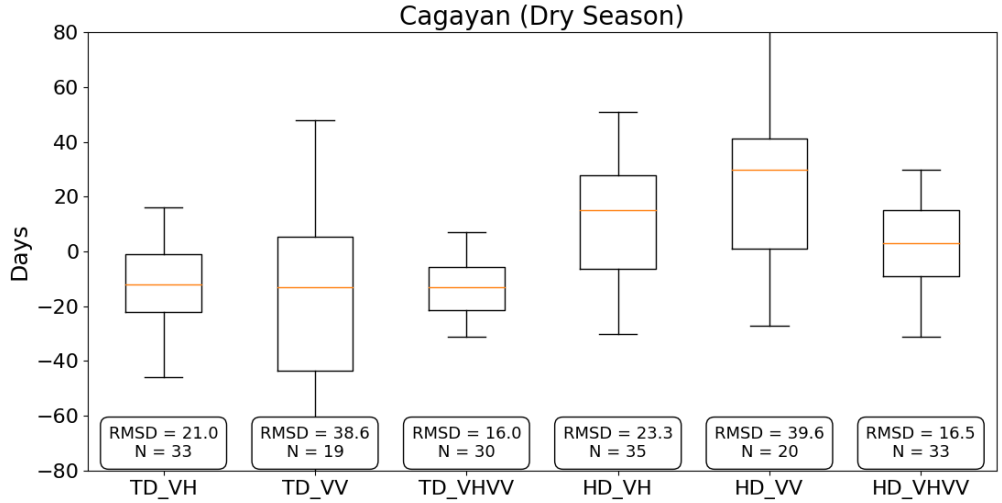

Figure 4.20 Boxplots of the temporal difference between the farmer-reported and detected transplanting and harvest dates in Cagayan during the dry season

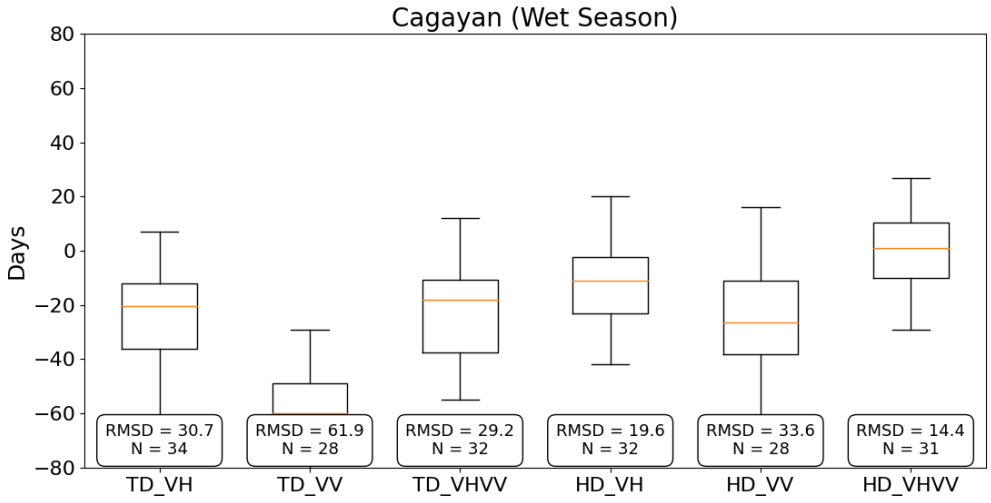

Figure 4.21 Boxplots of the temporal difference between the farmer-reported and detected transplanting and harvest dates in Cagayan during the wet season

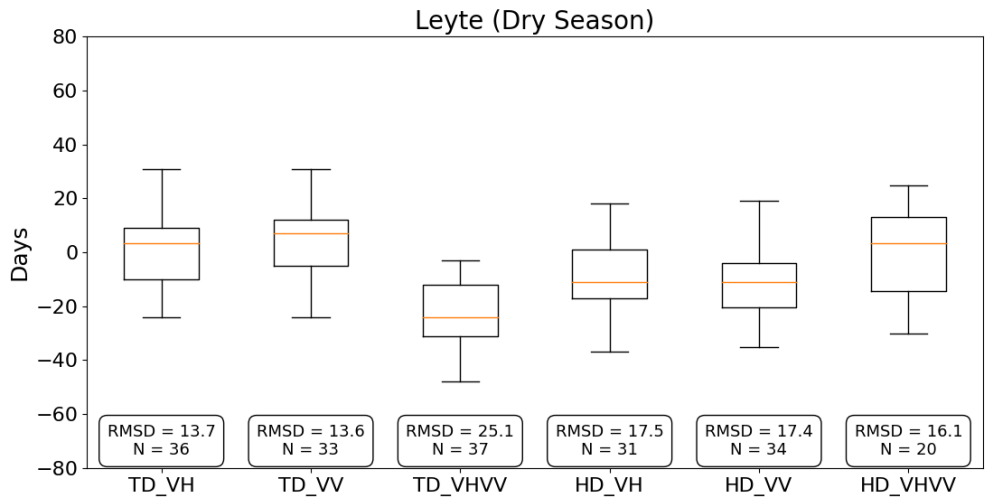

Figure 4.22 Boxplots of the temporal difference between the farmer-reported and detected transplanting and harvest dates in Leyte during the dry season

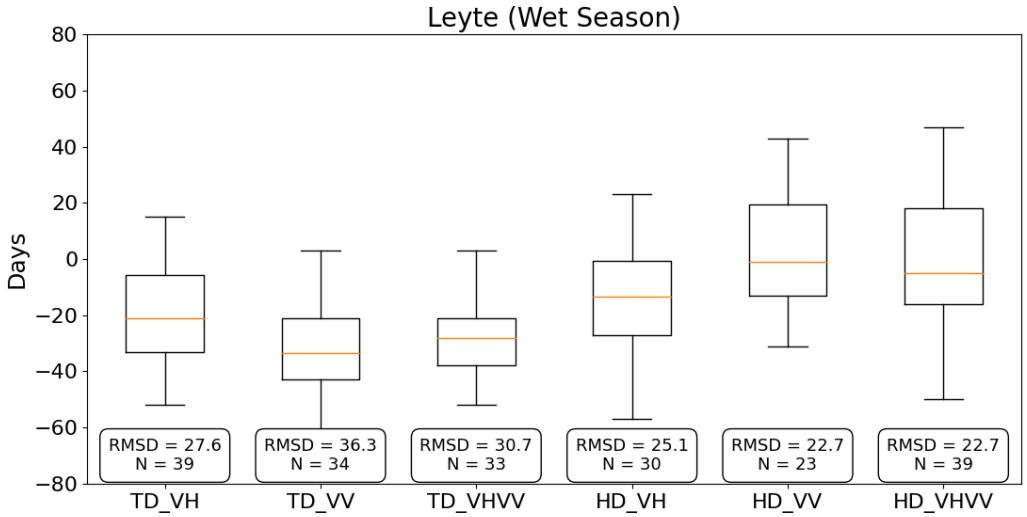

Figure 4.23 Boxplots of the temporal difference between the farmer-reported and detected transplanting and harvest dates in Leyte during the wet season

The maps of the rice fields in Leyte province during the dry season were generated to highlight the temporal difference between the farmer-reported and detected dates in VV polarization (Figure 4.24 and Figure 4.25).

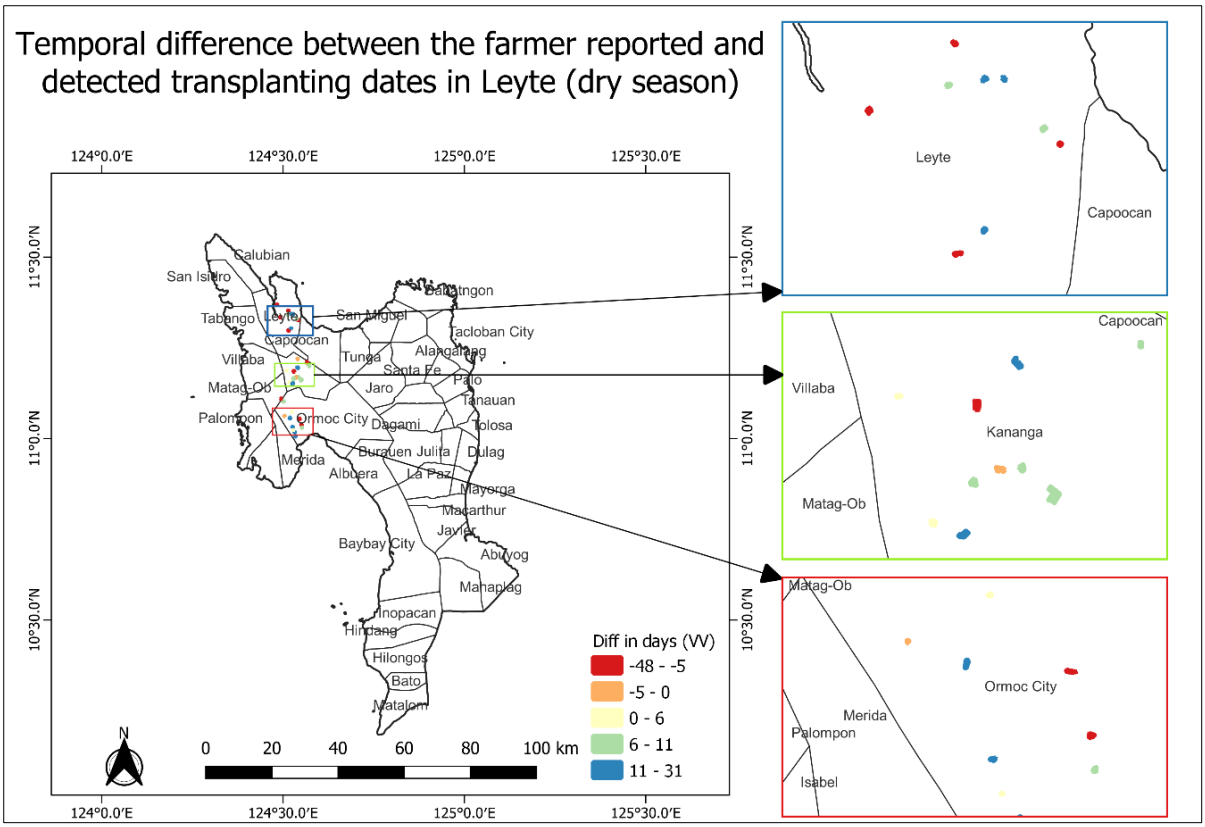

Figure 4.24 Temporal difference between the farmer-reported and detected transplanting dates in Leyte for VV polarization during the dry season

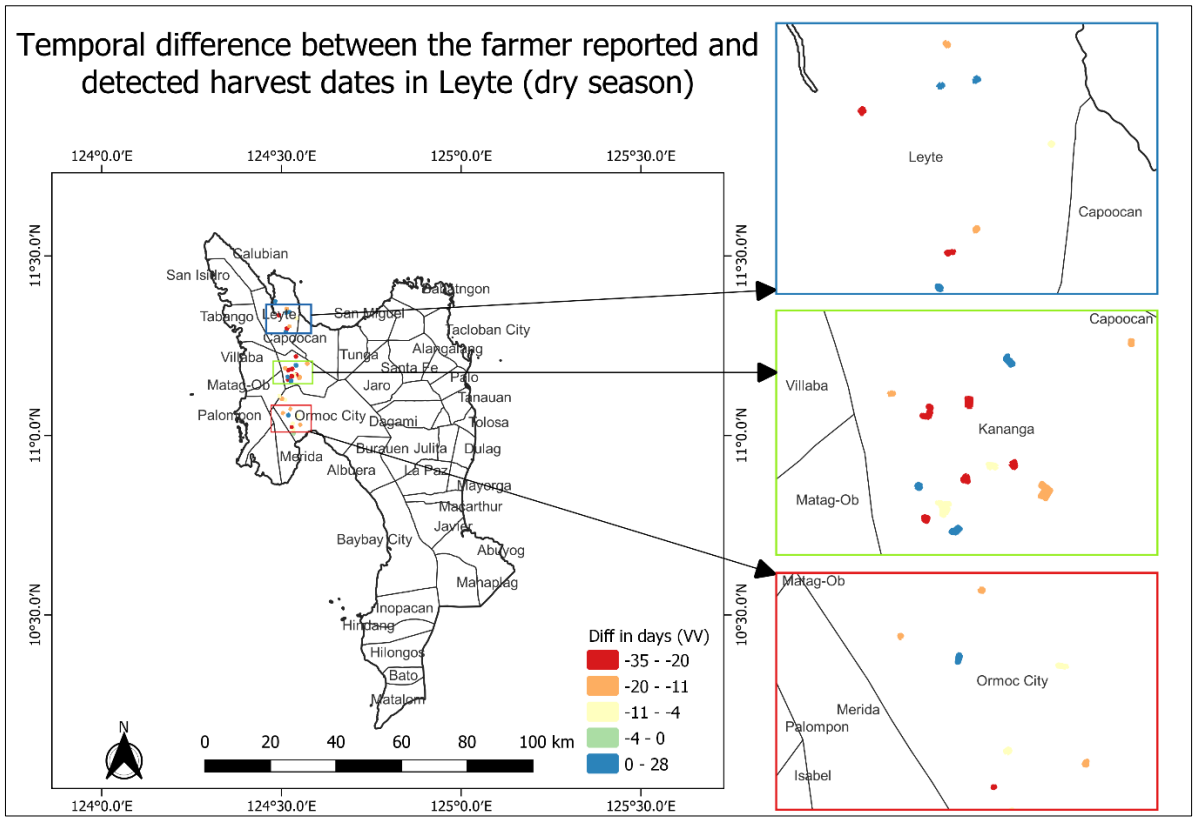

Figure 4.25 Temporal difference between the farmer-reported and detected harvest dates in Leyte for VV polarization during the dry season

5. DISCUSSION

Estimating transplanting and harvest dates of rice crops in the Philippines using Sentinel-1 data is of utmost relevance in enhancing agricultural productivity, food security, and climate resilience. This study aimed to leverage multi-temporal Sentinel-1 SAR data to determine the timing of rice crop transplanting and harvest, contributing to efficient agricultural planning and effective resource management. Hence, the study utilized the LOWESS function fitting technique to smoothen the time series curves, along with statistical techniques like periodogram analysis and the Breusch-Godfrey white noise tests for characterizing the temporal pattern, and local extrema extraction for detecting the transplanting and harvest dates. The results showed that VH and VV polarizations were useful in determining the transplanting and harvest dates of rice crops during the dry season, while VH/VV polarization demonstrated potential in estimating these dates mainly during the wet season.

The following sections discuss the integration of Sentinel-1A and Sentinel-1B data, evaluate the performance of the LOWESS smoothing technique, describe the significance of periodogram and Breusch-Godfrey test, emphasize the importance of identifying local extrema, and examine the spatial and temporal transferability of the method. Furthermore, limitations, implications and recommendations are also discussed.

5.1. Integration of Sentinel-1A and Sentinel-1B data

The provided Sentinel-1A time series data was validated by comparing the backscatter coefficients extracted from GEE to ensure data consistency and coherence when combined with Sentinel-1B data, which was also extracted from GEE. Sentinel-1A and Sentinel-1B are part of the same Sentinel-1 mission, designed to acquire data with similar imaging characteristics (Gorelick et al., 2017). GEE offers access to pre-processed Sentinel-1 data that has undergone calibration and standard processing steps to ensure data consistency and quality (Google Earth Engine Developers, 2022). These processing steps aim to normalize the data and maintain the original imaging geometry (Gorelick et al., 2017). Consequently, when processing Sentinel-1A and Sentinel-1B data through GEE, different imaging geometries, such as incidence angles and look directions, were expected to be comparable between the two satellites. The presence of a zigzag pattern in the time series curve (Figure 4.1) was more likely attributed to temporal differences, which refer to changes in the scattering properties of the Earth's surface over time (Ma et al., 2018). Temporal differences can introduce variations in the backscatter values, influencing the observed zigzag pattern.

Sentinel-1B played a critical role in augmenting SAR data alongside Sentinel-1A. However, due to an anomaly in its instrument electronics power supply, Sentinel-1B was incapable of transmitting radar data in December 2021 and was subsequently decommissioned (European Space Agency, 2022). Consequently, the unavailability of Sentinel-1B has resulted in a decreased pool of SAR data for various research endeavors. This reduction could have implications for the temporal coverage of analyses, particularly if there are gaps or restrictions in the dataset solely from Sentinel-1A. The absence of Sentinel-1B data may lead to a shorter time series or restricted observations during specific periods, potentially compromising the precision and dependability of the outcomes.

5.2. Performance of the LOWESS function fitting technique

The results unveiled the dominant optimal fraction parameters for each province, season, and polarization in the study (Table 4.1). Among all VH polarizations, a fraction parameter of 0.3 was identified as the most optimal. However, for VV and VH/VV polarizations, the dominant optimal fraction parameters varied based on the specific season and study area, with values of 0.3 and 0.5 being the primary choices. The selected values were optimal for reducing noise and fluctuations, allowing for identifying meaningful

patterns while preserving important details within the time series data. These findings are crucial for understanding the appropriate smoothing level required for accurately estimating transplanting and harvest dates.

The variability in optimal fraction parameters for different polarizations suggests that different smoothing requirements are necessary to capture the unique characteristics of these polarizations in different contexts. The choice of specific values as the primary optimal fraction parameters suggests a careful balance between achieving smoothness across the data and maintaining the ability to detect and capture local variations (Derkacheva et al., 2020). These highlight the importance of considering the specific characteristics of each polarization and the context of the study area when determining the optimal fraction parameter. By adopting the fraction parameter to the specific conditions, researchers can ensure the most accurate estimation of transplanting and harvest dates. These findings provide valuable guidance for practitioners and researchers working with Sentinel-1 time series data for rice crops. By understanding the dominant optimal fraction parameters for each province, season, and polarization, they can effectively apply LOWESS smoothing techniques to improve the accuracy of estimating important agricultural events, ultimately contributing to enhanced agricultural planning and management.

The goodness of fit between the original and LOWESS-smoothed time series curve was evaluated using the R^2. The analysis of the R^2 values revealed interesting trends and patterns. Specifically, it was observed that the VV data during the wet season generally exhibited the lowest R^2 values. A wider dispersion of R^2 values for VV polarization was observed in Agusan del Sur and Leyte provinces during the wet season, indicating greater variability in the goodness of fit compared to the Cagayan province. On the other hand, the VH data predominantly showcased the highest R^2 values among the three polarizations. This implies stronger linear relationships between the original and LOWESS-smoothed time series curve for VH polarization across all three provinces.

The observed trends in the R^2 values between the original and fitted time series curves across all polarizations during different seasons and provinces can be influenced by several factors, including vegetation characteristics, weather conditions, and land cover variability. VV polarization is more sensitive to the vertical structure and orientation of the crops at the early stage before the heading stage (Nasirzadehdizaji et al., 2019). During the wet season, rice crops may exhibit greater variability due to factors like water availability, growth stage, and variations in agricultural practices (Kushwaha et al., 2022). The complex arrangement of vegetation and water surfaces in rice fields can lead to increased variability in the backscatter response for VV polarization, leading to lower R^2 values for VV polarization. On the other hand, VH polarization can penetrate the vegetation canopy (Nguyen et al., 2016). This stronger penetration capability of VH polarization allows for better capture of the temporal trends and variations in the rice crop growth, resulting in higher R^2 values. The stronger linear relationships between the original and fitted time series curves in VH polarization indicate that the LOWESS smoothing technique effectively captures the dominant patterns in VH polarization, leading to higher accuracy in estimating the transplanting and harvest dates. Weather conditions also play a role, as the wet season is characterized by higher precipitation, humidity, and cloud cover. These environmental factors can impact the backscattered radar signal and introduce additional noise or interference in the VV polarization data (Harfenmeister et al., 2019). The moisture, vegetation canopies, and atmospheric effects during this season may contribute to a weaker correlation between the original and fitted curves, resulting in lower R^2 values for VV polarization. Regarding land cover variability, it is likely that Agusan del Sur and Leyte provinces exhibit more diverse land cover types and agricultural practices compared to the Cagayan province. Variations in soil properties, crop types, and cultivation methods can introduce additional complexity and heterogeneity in the VV polarization data (Nasirzadehdizaji et al., 2019). This spatial variability in land cover could lead to a wider dispersion of R^2 values for VV polarization in Agusan del Sur and Leyte provinces during the wet season, as the LOWESS smoothing may have varying degrees of accuracy across different land cover types (Plotnikov et al., 2022).

5.3. Significance of periodogram and Breusch-Godfrey test

The utilization of periodogram analysis has been instrumental in detecting and validating the existence and quantity of periodic components within a time series, representing recurring patterns (Hamilton, 2005). In this study, the periodogram served as a valuable tool for examining the seasonal patterns or cycles associated with the growth of rice crops. Applying the periodogram to the LOWESS-smoothed time series curve, prominent frequencies corresponding to the periodicity of rice crop phenology, including transplanting and harvest cycles, were identified. This analysis facilitated the determination of whether a single or double cycle occurred during the crop's growth period within the LOWESS-smoothed time series. Identifying dominant frequencies helped determine the number of local extrema (Palacios-Orueta et al., 2012). For example, a time series characterized by a dominant frequency of a single period or cycle exhibited one local minimum and one local maximum (Figure 5.1), while a time series with a dominant frequency of a double cycle (Figure 5.2) displayed at least two identical local extrema (either two local minima or two local maxima).

The BG test is a statistical procedure employed to assess the presence of autocorrelation within a regression model (Breusch, 1978; Godfrey, 1978). This test allows to verify whether a significant correlation exists among the residuals at various time lags, indicating the existence of repetitive patterns or cycles in the data (Edgerton & Shukur, 2007). Following identifying dominant frequencies or periodic patterns through periodogram analysis of the rice crop data, the BG test was implemented to determine the statistical significance and autocorrelation of these patterns. If the p-value of the time series data is statistically significant at a significance level of 0.05, the null hypothesis, which assumes the absence of systematic patterns, autocorrelation, and periodic components in the time series data, is rejected (Fuller, 1996). This enhanced the reliability of the findings and provided confirmation regarding the presence of repetitive patterns in the data. The time series data in Figure 5.1 and Figure 5.2 yielded statistically significant p-values at a significance level of 0.05. Consequently, these significant outcomes indicate that the analyzed data exhibited characteristics of non-white noise, suggesting the existence of discernible patterns rather than randomness. In cases where the null hypothesis is accepted, indicating a random pattern in the time series, the identified local extrema were further away from the farmer-reported dates.

By combining periodogram analysis for pattern identification and the BG test for confirming their significance and autocorrelation, a comprehensive approach is established to validate the presence and quantity of local extrema within the time series. These steps are instrumental in the subsequent procedures involved in estimating the transplanting and harvest dates of rice crops.

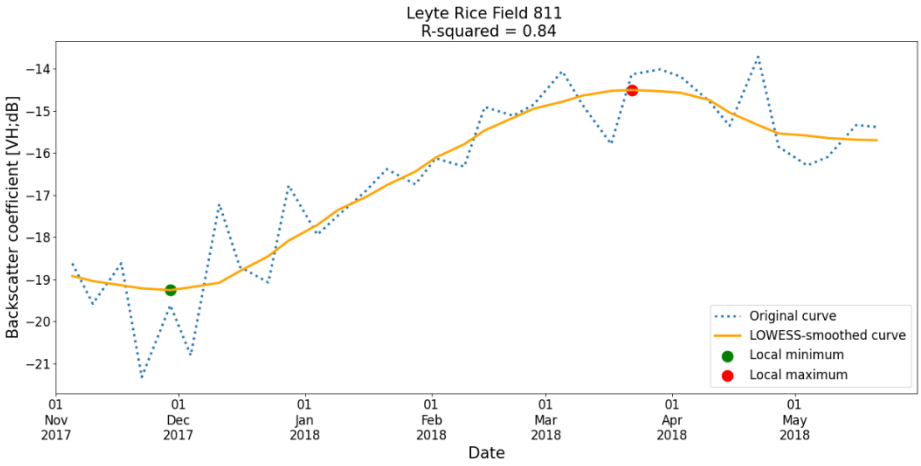

Figure 5.1 Original and LOWESS-smoothed time series curves of rice field 811 in Leyte in VH polarization during the dry season

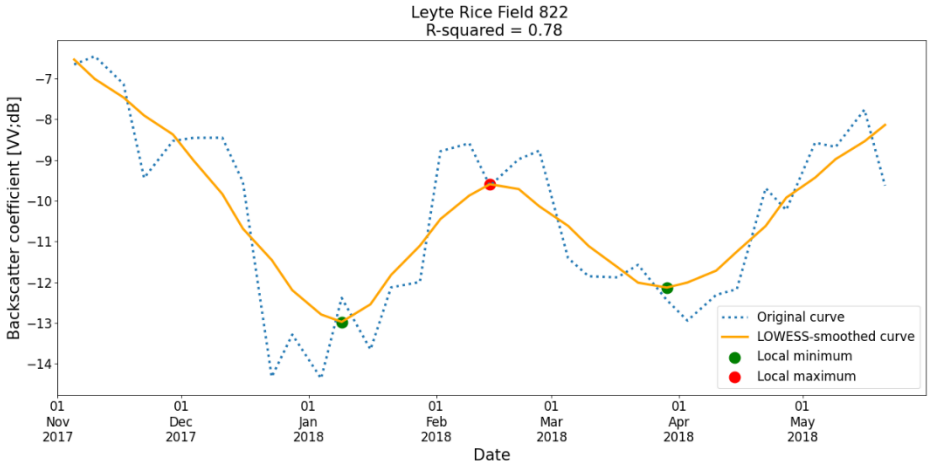

Figure 5.2 Original and LOWESS-smoothed time series curves of rice field 822 in Leyte in VV polarization during the dry season

5.4. Relative importance of local extrema

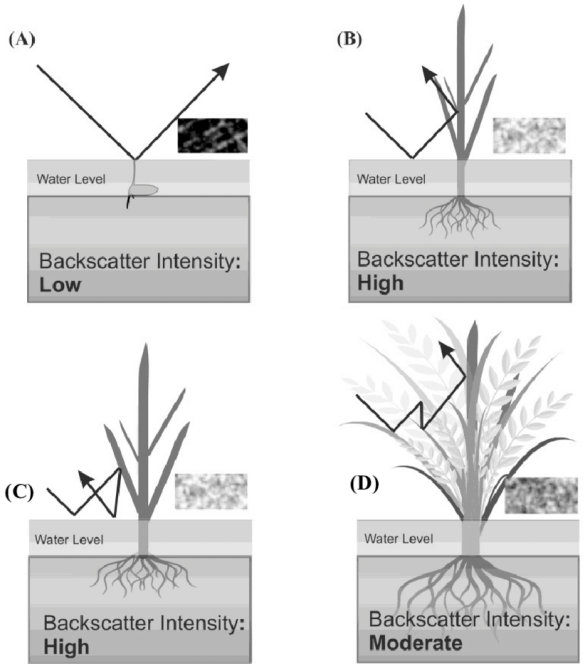

Figure 5.3 Sentinel-1 backscatter mechanisms during different growth stages of rice and example of the resulted backscatter intensities in C-band. Source: (Arjasakusuma et al., 2021)

Rice cultivation typically occurs in flooded fields, where standing water leads to specular reflection and lowers the backscatter coefficients (Chen & Mcnairn, 2006). Consequently, a discernable temporal pattern was observed in the time series curve, reflecting a trend of decreasing backscatter coefficients as the transplanting period approaches and remains low until the early tillering phase with water still present (Mandal et al., 2018). During the transplanting period, the backscatter coefficients notably decreased due to the dominant backscatter mechanism of specular reflection (Figure 5.3 (A)) on the water surface, resulting in minimal backscatter. Consequently, most of the low backscatter coefficients were observed around the transplanting period (Figure 4.9, Figure 4.10 and Figure 4.11). Hence, local minimum points in the backscatter coefficients corresponded to the lowest intensity values, suggesting the transplanting period.

The growth rate of rice crops can vary depending on various factors, including weather conditions, crop management practices, and rice varieties (Boonwichai et al., 2018; Yoshida, 1981). The comparison between the transplanting and harvest dates obtained from field information and the detected dates (Figure 4.18 to Figure 4.23) revealed that most local minimum values occurred a few days after the farmer-reported transplanting dates. This can be attributed to the initial stages after transplanting when the plants are small and have low biomass, resulting in relatively low backscatter coefficients (Vreugdenhil et al., 2018). The growth process may also take some time, causing the lowest backscatter values to occur after the transplanting date. Additionally, some of the detected transplanting dates that do not closely align with the farmer-reported transplanting dates were likely impacted by flooding or excessive water during the tillering or early stages of rice growth, leading to low backscatter coefficients of water surface on that date (Phan et al., 2021).

The harvest period for rice crops in the Philippines typically occurs between 100-110 days after transplanting, depending on the specific growth duration of the rice variety (IRRI, 2013). In this study, the plots for VH and VH/VV polarizations (Figure 4.9 and Figure 4.11) demonstrated that the local maximum detected after the local minimum can be associated with the rice crop's harvest dates. Similarly, for VV polarization, the second local maximum following the local minimum can be linked to the harvest dates (Figure 4.10). However, in cases where there is only one local maximum for VV polarization, the date of its occurrence of the local maximum was considered as the detected harvest date.

As the rice plants grow and become more densely vegetated, there is an increase in backscatter coefficients. Following the rice harvest, the backscatter coefficients are anticipated to decrease significantly as the contribution from the canopy becomes negligible (Clauss et al., 2018). However, the results indicated that the backscatter coefficients remained relatively high and most of the local maxima were observed after the farmer-reported harvest dates (Figure 4.18 to Figure 4.23). This indicates that the backscatter coefficients continued to rise even after the harvest dates. Mandal et al. (2018) suggested that this phenomenon may be attributed to the prevalent use of machine harvesting in the area, where a substantial amount of rice stubble and straw is left on the fields. Field survey data confirmed that a considerable proportion of rice fields utilized machine harvesters, and the practice of allowing rice stubbles to decompose on the fields was widespread in the study area. Consequently, the total backscatter power is influenced by the volume scattering component originating from the harvested rice field (Mandal et al., 2018).

5.5. Spatial and temporal transferability

The method employed in this study demonstrated its capability of performing in different seasons and spatial locations. However, the number of extracted Sentinel-1 data varied spatially and temporally due to differences in satellite coverage and frequency of passes by the Sentinel-1 mission (Canty et al., 2019). The orbital pattern followed by Sentinel-1 satellites affects data availability, with some areas having more frequent satellite passes and a larger number of available data. These orbital passes vary across seasons, leading to variations in the timing and coverage of captured Sentinel-1 images depending on the specific area of interest (Potin et al., 2016). Consequently, there can be variability in the number of available Sentinel-1 images, as indicated by the difference in the extracted Sentinel-1 data (Table 2.2 and Table 2.3). This variation is dependent on the specific province and the season being considered.

The estimation of transplanting and harvest dates exhibited variations influenced by factors such as polarization type, season, and geographic location of rice fields. The backscatter coefficients of rice crops are affected by environmental elements like rainfall, soil moisture, and temperature (Veloso et al., 2017). The effect of water presence on Sentinel-1 radar polarization varies between VV and VH polarizations, with VV polarization being more susceptible (Tsyganskaya et al., 2019). In the wet season, rice fields often have standing water due to rainfall or irrigation, which can result in specular reflections in the backscatter signal (Arjasakusuma et al., 2021). These reflections from the water surface can introduce additional noise and fluctuations in the backscatter time series. The wet season is characterized by higher soil moisture content in rice fields due to precipitation and irrigation, which can enhance volume scattering and surface roughness, thereby influencing the backscatter signal (Ullmann et al., 2023). Conversely, during the dry season, the minimal presence of standing water creates a smoother and more uniform surface, resulting in reduced noise and fluctuations in the backscatter signal. Additionally, soil moisture levels tend to be lower during the dry season, resulting in reduced volume scattering and a more stable backscatter time series (Ullmann et al., 2023). Furthermore, rice crops undergo rapid growth during the wet season, leading to increased vegetation density and height (Yang et al., 2008). The dense canopy and taller plants during this period contribute to more variability in backscatter due to the presence of multiple scattering mechanisms, such as volume scattering from vegetation layers, surface scattering from standing water, and double-bounce scattering from vegetation and water interactions (Clauss et al., 2018). These multiple scattering mechanisms contribute to higher noise levels and fluctuations in the backscatter signal.

The application of the MAD technique resulted in varying numbers of outlier rice fields that were not considered for final assessment, depending on the season and location (Table 4.4). In some cases, the number of rice fields used for comparing the farmer-reported and detected transplanting dates differed from those used for comparing the farmer-reported and detected harvest dates. This variation occurred due to certain rice fields not exhibiting local minimum or maximum values or being identified as outliers.

During the dry season in Agusan del Sur, the VH and VV polarizations showed the lowest RMSD values of 12.4 and 9.2 days, respectively, for transplanting dates, indicating more accurate results with less scattering (Figure 4.18). VH polarization also displayed the lowest RMSD values of 17.5 days for harvest dates. However, most of the detected transplanting and harvest dates were later than the farmer-reported dates. In the wet season, VH/VV polarization exhibited the lowest RMSD values of 14.7 and 8.8 days for transplanting and harvest dates, respectively, and showed less scattered results (Figure 4.19). Similarly, most of the detected transplanting dates occurred later than the farmer-reported dates, while the majority of detected harvest dates occurred earlier.

During the dry season in Cagayan province, VH/VV polarization demonstrated the lowest RMSD values of 16 and 16.5 days for transplanting and harvest dates, respectively, and showed less scattered data points, indicating a higher level of precision (Figure 4.20). However, most of the detected transplanting dates were later than the farmer-reported dates, while most harvest dates occurred earlier than the farmer-reported dates. In contrast, during the wet season, the detected transplanting dates for all polarizations substantially deviated from the farmer-reported dates, with RMSD values exceeding 20 days (Figure 4.21) . Nevertheless, VH/VV polarization outperformed other polarizations by exhibiting the lowest RMSD values of 14.4 days for harvest dates.

In Leyte province during the dry season, VH and VV polarizations demonstrated the lowest RMSD values of 13.7 and 13.6 days, respectively, for transplanting dates, considering data from over 30 rice fields (Figure 4.22). The harvest dates showed close RMSD values of 17.5, 17.4, and 16.1 days for VH, VV, and VH/VV polarizations, respectively, with similar spread of results across all polarizations. The detected transplanting dates tended to be earlier than the farmer-reported dates, while the detected harvest dates tended to be later. However, during the wet season, all polarizations exhibited higher RMSD values exceeding 20 days for both transplanting and harvest dates, indicating greater variability (Figure 4.23). These findings provide valuable insights into the accuracy of detecting transplanting and harvest dates for rice crops using different polarizations, emphasizing the seasonal and regional variations involved.

Generally, the RMSD values for VH and VH/VV polarizations remained consistent within a 30-day range across all three provinces and seasons. However, for VV polarization during the wet season, the RMSD values varied. Specifically, the RMSD values for Agusan del Sur, Cagayan, and Leyte were 45 days, 61 days, and 36 days, respectively. These findings highlight the potential of utilizing different polarizations to estimate rice crops' transplanting and harvest dates in dry and wet seasons. Specifically, the VH and VV polarizations have shown to be particularly valuable during the dry season in Agusan del Sur and Leyte provinces. Additionally, the VH/VV polarization has demonstrated promising outcomes for estimating transplanting and harvest dates during the wet season in these provinces. In the case of Cagayan province, the VH/VV polarization has exhibited favorable results for both dry and wet seasons, indicating the effectiveness in estimating transplanting and harvest dates throughout the year.

The variation in the outcomes is associated with the geographical placement of the rice fields, as the diverse climate conditions can impact the backscatter coefficients of the rice crops (Veloso et al., 2017). Crop growth relies on various factors, including climatic conditions (Pang et al., 2021). The three provinces under investigation exhibited distinct climatic conditions, despite their geographical proximity within the same country (Figure 2.1). Agusan del Sur predominantly has a type II climate, while Cagayan experiences a mix of types III and IV climates, and Leyte has a dominant type IV climate (Basconcillo et al., 2018).

This study emphasized the importance of considering seasonal and regional variations when utilizing different polarizations to detect transplanting and harvest dates for rice crops. These insights can inform decision-making processes in agriculture and help optimize resource allocation in rice-growing regions.

5.6. Limitations

The study has showcased the promising capability of Sentinel-1 time series SAR data in estimating rice crops' transplanting and harvest dates. However, it is important to acknowledge certain limitations observed during the study, which may restrict the generalizability of the findings beyond the specific study conditions. One such limitation was the limited number of samples available for the analysis. Specifically, the analysis included 19 rice fields for Agusan del Sur, 38 rice fields for Cagayan and 42 rice fields for Leyte. The size of the dataset or the number of samples can impact the generalizability and statistical robustness of the findings (Schloss, 2018). A small sample size may introduce bias and limit the representativeness of the results, potentially affecting the accuracy and reliability of the transplanting and harvest date estimations.

Another limitation of this study was that the provided transplanting and harvest dates were indicated by the respective week of the month instead of the exact dates. Consequently, the farmer-reported transplanting and harvest dates were assumed to take place in the middle of the week, specifically on the 4th, 11th, 18th or 25th day of the month. This assumption affects the accuracy of the estimation since the actual dates could vary on other days within the week. Furthermore, variations arise from the presence or absence of information regarding different management practices in various rice fields, making it challenging to identify the underlying reasons for the observed discrepancies. Future field survey data for this type of study should ideally include exact dates for the actual transplanting and harvest events, as well as other relevant information such as management practices.

Considering the limitations of remote sensing data such as Sentinel-1 SAR data is crucial. Like other remote sensing data, Sentinel-1 SAR data have their own limitations, such as data gaps, spatial and temporal resolution, and environmental factors (Fernández et al., 2022). In this study, the time interval of the Sentinel-1 data was set at six days. However, it is important to note that there were instances where the interval was inconsistent due to missing data on specific dates, especially during the wet season. This inconsistency in the data availability can introduce uncertainties and limitations in the analysis of transplanting and harvest dates. Furthermore, the acquisition dates of Sentinel-1 data varied across the different provinces. This variation applied to both Sentinel-1A and Sentinel-1B data. The temporal offset between the data acquisition dates can potentially impact the accuracy and reliability of the estimations, as the conditions of the rice crops may vary between acquisition dates. To mitigate these limitations, it is important to carefully consider the availability and consistency of the data when interpreting the results. Additionally, future studies could explore strategies to address the temporal inconsistencies, such as data interpolation or gap-filling techniques, to ensure a more continuous and consistent dataset for estimating transplanting and harvest dates.

5.7. Implications

The estimation of transplanting and harvest dates of rice crops in the Philippines has significant implications for agricultural planning and management. Farmers and policymakers can make informed decisions to optimize crop production and improve agricultural practices by accurately determining these critical dates. Some specific implications of this research are:

1. Improved crop planning: Accurate estimation of transplanting and harvest dates allows farmers to plan their cultivation activities more effectively. They can align their planting schedules, irrigation management, and pest control strategies based on the estimated dates, leading to better crop yields and resource utilization.

2. Efficient resource allocation: Knowing the transplanting and harvest dates helps optimize the allocation of resources such as fertilizers, water, labor, and machinery. Farmers can adjust their resource inputs based on the crop's growth stage, ensuring efficient resource utilization and minimizing waste.
3. Improved risk management: Estimating transplanting and harvest dates can contribute to better risk management in agriculture. Farmers can anticipate and mitigate potential risks associated with weather events, pests, diseases, or market fluctuations by aligning their management practices and decision-making with the detected crop growth stages.
4. Policy and government support: The findings of this study can inform agricultural policies and government support programs. Accurate estimation of transplanting and harvest dates can aid in the formulation of policies related to crop insurance, subsidies, and market interventions. It provides a scientific basis for decision-makers to support and promote sustainable agricultural practices.
5. Future research could explore the possibilities of utilizing Sentinel-1 SAR data alongside recent field survey data to forecast transplanting and harvest dates. The current findings support the use of Sentinel-1 SAR data in estimating these critical dates. With adequate historical Sentinel-1 SAR data and up-to-date field survey information, it may be feasible to develop forecasting models for transplanting and harvest dates.

Overall, the implications of this study contribute to the advancement of agricultural planning, resource management, and decision-making processes. The accurate estimation of transplanting and harvest dates for rice crops can lead to improved productivity, profitability, and sustainability in the agricultural sector of the Philippines.

5.8. Recommendations

Based on the findings of this study, the following recommendations are proposed further to enhance the application and impact of the research:

1. Integration of additional data sources: To enhance the accuracy and reliability of transplanting and harvest date estimations, consider integrating additional data sources such as weather data, soil information, or satellite imagery. This can provide valuable insights into environmental conditions and crop growth stages, contributing to more robust and precise estimations. Furthermore, a greater amount of historical time series data is required to predict transplanting and harvest dates. The availability of extensive data records enhances the overall reliability of the estimations.
2. Enhance field survey data: In future studies, it is advisable to collect field survey data that includes exact dates for the actual transplanting and harvest events and other relevant information like specific management practices employed by farmers. Collaborating with farmers, agricultural experts, and local stakeholders will facilitate the collection of ground truth data, enabling a more comprehensive validation of the estimated dates and enhancing the reliability of the results.
3. Expansion to Different Provinces: Consider extending the research to other provinces in the Philippines, especially those with distinct climate types - not covered in this study. This would allow for a broader understanding of the applicability and effectiveness of the methodology across different regions, enhancing its generalizability and practical utility.

6. CONCLUSION

This research has explored the use of Sentinel-1 SAR data to estimate the transplanting and harvest dates of rice crops in the Philippines. The analysis focused on two distinct seasons, the dry season and the wet season, in three provinces of the Philippines: Agusan del Sur, Cagayan, and Leyte.

The coefficient of determination (R^2) was used to evaluate the agreement between the original and LOWESS-smoothed time series curve, revealing interesting trends and patterns. Notably, VV data during the wet season consistently displayed the lowest R^2 values. A wider range of R^2 values for VV polarization was observed in the Agusan del Sur and Leyte provinces, indicating greater variability in the goodness of fit compared to the Cagayan province. Conversely, the VH data consistently exhibited the highest R^2 values among the three polarizations, indicating stronger linear relationships between the original and fitted time series curves for VH polarization across all three provinces.

During the transplanting period of rice crops, there is a significant decrease in backscatter coefficients due to the dominant backscatter mechanism of specular reflection on the water surface. This results in minimal backscatter, as observed in the low backscatter coefficients around the transplanting period. The growth rate of rice crops is influenced by various factors, such as weather conditions, crop management practices, and rice varieties. Comparing the farmer-reported dates of transplanting and harvest obtained from field information with the detected dates revealed that most of the local minimum values occurred a few days after the transplanting period. This delay can be attributed to the initial stages after transplanting when the plants are small and have low biomass, leading to low backscatter coefficients.

The analysis revealed that for VV polarization, some harvest dates were linked to the first local maximum after the first local minimum, while others were linked to the second local maximum following the first local minimum. In contrast, for VH and VH/VV polarizations, the harvest dates consistently corresponded to the local maximum immediately after the first local minimum. It is worth noting that certain rice fields may not display a local maximum due to factors such as retaining rice stubbles or implementing ratooning techniques. The number of rice fields used for comparing farmer-reported and detected transplanting dates differed from those used for comparing harvest dates. This variation was due to rice fields not exhibiting local minimum or maximum values or being identified as outliers. The evaluation of the RMSD values indicated the potential of using different polarizations for estimating transplanting and harvest dates in both dry and wet seasons. VH and VV polarizations were particularly valuable during the dry season in Agusan del Sur and Leyte provinces, while VH/VV polarization showed promising outcomes for estimating dates in wet seasons. In Cagayan province, VH/VV polarization demonstrated effectiveness throughout the year. The variations in outcomes can be attributed to the geographical placement of rice fields and the diverse climate conditions that impact the backscatter intensities of rice crops. The different climatic conditions experienced by Agusan del Sur, Cagayan, and Leyte provinces contributed to the variations in results.

Overall, this research has significant implications for the agricultural sector in the Philippines. Leveraging remote sensing and data-driven approaches presents opportunities to optimize crop management practices, allocate resources effectively, and support sustainable rice production. Implementing the recommendations and addressing the challenges highlighted in this study can maximize its impact, fostering the advancement of precision agriculture and promoting socio-economic development in agricultural communities of the Philippines.

7. REFERENCES

Andrade, C. (2020). Mean Difference, Standardized Mean Difference (SMD), and Their Use in Meta-Analysis: As Simple as It Gets. *The Journal of Clinical Psychiatry*, *81*(5), 11349. https://doi.org/10.4088/JCP.20F13681

Arjasakusuma, S., Kusuma, S. S., Mahendra, W. K., & Astriviany, N. (2021). Mapping paddy field extent and temporal pattern variation in a complex terrain area using sentinel 1-time series data: Case study of magelang district, indonesia. *International Journal of Geoinformatics*, *17*(2), 79–88. https://doi.org/10.52939/IJG.V17I2.1763

Aulard-Macler, M. (2011). *Sentinel-1 Product definition*.

Basconcillo, J., Lucero, A., Solis, A., Sandoval, R., Bautista, E., Koizumi, T., & Kanamaru, H. (2018). Statistically downscaled projected changes in seasonal mean temperature and rainfall in Cagayan Valley, Philippines. *Journal of the Meteorological Society of Japan*, *94A*, 151–164. https://doi.org/10.2151/JMSJ.2015-058

Boonwichai, S., Shrestha, S., Babel, M. S., Weesakul, S., & Datta, A. (2018). Climate change impacts on irrigation water requirement, crop water productivity and rice yield in the Songkhram River Basin, Thailand. *Journal of Cleaner Production*, *198*, 1157–1164. https://doi.org/10.1016/J.JCLEPRO.2018.07.146

Braun, A. (2021). Retrieval of digital elevation models from Sentinel-1 radar data - Open applications, techniques, and limitations. *Open Geosciences*, *13*(1), 532–569. https://doi.org/https://doi.org/10.1515/geo-2020-0246

Breusch, T. S. (1978). TESTING FOR AUTOCORRELATION IN DYNAMIC LINEAR MODELS*. *Australian Economic Papers*, *17*(31), 334–355. https://doi.org/10.1111/J.1467-8454.1978.TB00635.X

Cabunagan, R. C., Castilla, N., Coloquio, E. L., Tiongco, E. R., Truong, X. H., Fernandez, J., Du, M. J., Zaragosa, B., Hozak, R. R., Savary, S., & Azzam, O. (2001). Synchrony of planting and proportions of susceptible varieties affect rice tungro disease epidemics in the Philippines. *Crop Protection*, *20*(6), 499–510. https://doi.org/10.1016/S0261-2194(01)00017-5

Canty, M. J., Nielsen, A. A., Conradsen, K., & Skriver, H. (2019). Statistical Analysis of Changes in Sentinel-1 Time Series on the Google Earth Engine. *Remote Sensing 2020, Vol. 12, Page 46*, *12*(1), 46. https://doi.org/10.3390/RS12010046

Chen, C., & Mcnairn, H. (2006). A neural network integrated approach for rice crop monitoring. *Http://Dx.Doi.Org/10.1080/01431160500421507*, *27*(7), 1367–1393. https://doi.org/10.1080/01431160500421507

Chumkesornkulkit, K., Kasetkasem, T., Rakwatin, P., Eiumnoh, A., Kumazawa, I., & Buddhaboon, C. (2013). Estimated rice cultivation date using an extended Kalman filter on MODIS NDVI time-series data. *2013 10th International Conference on Electrical Engineering/Electronics, Computer, Telecommunications and Information Technology, ECTI-CON 2013*. https://doi.org/10.1109/ECTICON.2013.6559573

Clauss, K., Ottinger, M., & Kuenzer, C. (2018). Mapping rice areas with Sentinel-1 time series and superpixel segmentation. *International Journal of Remote Sensing*, *39*(5), 1399–1420. https://doi.org/10.1080/01431161.2017.1404162/SUPPL_FILE/TRES_A_1404162_SM1735.PDF

Cleveland, W. S. (1979). Robust locally weighted regression and smoothing scatterplots. *Journal of the American Statistical Association*, *74*(368), 829–836. https://doi.org/10.1080/01621459.1979.10481038

Corcione, V., Nunziata, F., Mascolo, L., & Migliaccio, M. (2016). A study of the use of COSMO-SkyMed SAR PingPong polarimetric mode for rice growth monitoring. *International Journal of Remote Sensing*,

37(3), 633–647. https://doi.org/10.1080/01431161.2015.1131902

Cota, N., Kasetkasem, T., Rakwatin, P., Chanwimaluang, T., & Kumazawa, I. (2015). Rice phenology estimation based on statistical models for time-series SAR data. *ECTI-CON 2015 - 2015 12th International Conference on Electrical Engineering/Electronics, Computer, Telecommunications and Information Technology*. https://doi.org/10.1109/ECTICON.2015.7207072

Dai, Y., Wang, Y., Leng, M., Yang, X., & Zhou, Q. (2022). LOWESS smoothing and Random Forest based GRU model: A short-term photovoltaic power generation forecasting method. *Energy*, *256*, 124661. https://doi.org/10.1016/J.ENERGY.2022.124661

Davidson, J. S. (2016). Why the Philippines Chooses to Import Rice. *Https://Doi.Org/10.1080/14672715.2015.1129184*, *48*(1), 100–122. https://doi.org/10.1080/14672715.2015.1129184

Derkacheva, A., Mouginot, J., Millan, R., Maier, N., & Gillet-Chaulet, F. (2020). Data Reduction Using Statistical and Regression Approaches for Ice Velocity Derived by Landsat-8, Sentinel-1 and Sentinel-2. *Remote Sensing 2020, Vol. 12, Page 1935*, *12*(12), 1935. https://doi.org/10.3390/RS12121935

Edgerton, D., & Shukur, G. (2007). Testing autocorrelation in a system perspective testing autocorrelation. *Http://Dx.Doi.Org/10.1080/07474939908800351*, *18*(4), 343–386. https://doi.org/10.1080/07474939908800351

Elamir, E. (2012). Mean Absolute Deviation about Median as a Tool of Explanatory Data Analysis. *IJRRAS*, *11*. https://www.researchgate.net/publication/266055577_Mean_Absolute_Deviation_about_Median_as_a_Tool_of_Explanatory_Data_Analysis

ESA. (2021). *Sentinel-1- Observation Scenario - Planned Acquisitions - ESA - Sentinel Online*. https://sentinels.copernicus.eu/web/sentinel/missions/sentinel-1/observation-scenario

European Space Agency. (2022). *Mission ends for Copernicus Sentinel-1B satellite*. https://www.esa.int/Applications/Observing_the_Earth/Copernicus/Sentinel-1/Mission_ends_for_Copernicus_Sentinel-1B_satellite

FAO. (2003). *Philippines[91]*. WTO Agreement on Agriculture: The Implementation Experience - Developing Country Case Studies. https://www.fao.org/3/Y4632E/y4632e0u.htm#fn91

FAO. (2017). *The future of food and agriculture | FAO | Food and Agriculture Organization of the United Nations*. Rome. https://www.fao.org/publications/fofa/en/

FAO. (2021). The State of Food Security and Nutrition in the World 2021. *The State of Food Security and Nutrition in the World 2021*. https://doi.org/10.4060/CB4474EN

FAO. (2022). *Philippines at a glance | FAO in the Philippines* . https://www.fao.org/philippines/fao-in-philippines/philippines-at-a-glance/en/

Fernández, M., Peter, H., Arnold, D., Duan, B., Simons, W., Wermuth, M., Hackel, S., Fernández, J., Jäggi, A., Hugentobler, U., Visser, P., & Féménias, P. (2022). Copernicus Sentinel–1 POD reprocessing campaign. *Advances in Space Research*, *70*(2), 249–267. https://doi.org/10.1016/J.ASR.2022.04.036

Fikriyah, V. N., Darvishzadeh, R., Laborte, A., Khan, N. I., & Nelson, A. (2019). Discriminating transplanted and direct seeded rice using Sentinel-1 intensity data. *International Journal of Applied Earth Observation and Geoinformation*, *76*, 143–153. https://doi.org/10.1016/J.JAG.2018.11.007

Fuller, W. A. (1996). *Introduction to statistical time series* (R. A. B. N. I. F. J. S. H. Vic Barnett, D. G. K. D. W. S. A. F. M. S. J. B. Kadane, & G. S. W. Jozef L. Teugels (eds.); 2nd ed.). JOHN WILEY & SONS, INC. . https://www.wiley.com/en-us/Introduction+to+Statistical+Time+Series%2C+2nd+Edition-p-9780471552390

Fushiki, T. (2011). Estimation of prediction error by using K-fold cross-validation. *Statistics and Computing*, *21*(2), 137–146. https://doi.org/10.1007/S11222-009-9153-8/METRICS

Godfrey, L. G. (1978). Testing for Higher Order Serial Correlation in Regression Equations when the Regressors Include Lagged Dependent Variables. *Econometrica*, *46*(6), 1303. https://doi.org/10.2307/1913830

Google Earth Engine Developers. (2022). *Sentinel-1 SAR data guide*. https://developers.google.com/earth-engine/guides/sentinel1

Gorelick, N., Hancher, M., Dixon, M., Ilyushchenko, S., Thau, D., & Moore, R. (2017). Google Earth Engine: Planetary-scale geospatial analysis for everyone. *Remote Sensing of Environment*, *202*, 18–27. https://doi.org/10.1016/J.RSE.2017.06.031

Gumbricht, T. (2016). Soil moisture dynamics estimated from MODIS time series images. *Remote Sensing and Digital Image Processing*, *20*, 233–253. https://doi.org/10.1007/978-3-319-47037-5_12/FIGURES/7

Gutierrez, M. A., Paguirigan, N. M., Raviz, J., Mabalay, M. R., Alosnos, E., Villano, L., Asilo, S., Arocena, A., Maloom, J., & Laborte, A. (2019). The Rice Planting Window in the Philippines: An Analysis Using Multi-Temporal SAR Imagery. *International Archives of the Photogrammetry, Remote Sensing and Spatial Information Sciences - ISPRS Archives*, *42*(4/W19), 241–248. https://doi.org/10.5194/ISPRS-ARCHIVES-XLII-4-W19-241-2019

Hamilton, J. D. (2005). *Time Series Analysis STANDARD/STATIC GRANGER CAUSALITY*. *3*, 1–85.

Harfenmeister, K., Spengler, D., & Weltzien, C. (2019). Analyzing Temporal and Spatial Characteristics of Crop Parameters Using Sentinel-1 Backscatter Data. *Remote Sensing 2019, Vol. 11, Page 1569*, *11*(13), 1569. https://doi.org/10.3390/RS11131569

He, Z., Li, S., Wang, Y., Dai, L., & Lin, S. (2018). Monitoring Rice Phenology Based on Backscattering Characteristics of Multi-Temporal RADARSAT-2 Datasets. *Remote Sensing 2018, Vol. 10, Page 340*, *10*(2), 340. https://doi.org/10.3390/RS10020340

Hossain, M. F., . M. A. S., . M. R. U., . Z. P., & . M. A. R. S. (2002). A Comparative Study of Direct Seeding Versus Transplanting Method on the Yield of Aus Rice. *Journal of Agronomy*, *1*(2), 86–88. https://doi.org/10.3923/JA.2002.86.88

Howell, D. C. (2005). Median Absolute Deviation. *Encyclopedia of Statistics in Behavioral Science*. https://doi.org/10.1002/0470013192.BSA384

Imran, M., Basit, I., Khan, M. R., & Ahmad, S. R. (2018). Analyzing the Impact of Spatio-Temporal Climate Variations on the Rice Crop Calendar in Pakistan. *International Journal of Agricultural and Biosystems Engineering*. https://doi.org/10.5281/ZENODO.1317168

IRRI. (2013). *Harvesting - IRRI Rice Knowledge Bank*. http://www.knowledgebank.irri.org/step-by-step-production/postharvest/harvesting

Jenkins, J. P., Braswell, B. H., Frolking, S. E., & Aber, J. D. (2002). Detecting and predicting spatial and interannual patterns of temperate forest springtime phenology in the eastern U.S. *Geophysical Research Letters*, *29*(24), 54–1. https://doi.org/10.1029/2001GL014008

Kushwaha, A., Dave, R., Kumar, G., Saha, K., & Khan, A. (2022). Assessment of rice crop biophysical parameters using Sentinel-1 C-band SAR data. *Advances in Space Research*, *70*(12), 3833–3844. https://doi.org/10.1016/J.ASR.2022.02.021

Lasko, K., Vadrevu, K. P., Tran, V. T., & Justice, C. (2018). Mapping Double and Single Crop Paddy Rice with Sentinel-1A at Varying Spatial Scales and Polarizations in Hanoi, Vietnam. *IEEE Journal of Selected Topics in Applied Earth Observations and Remote Sensing*, *11*(2), 498–512. https://doi.org/10.1109/JSTARS.2017.2784784

Li, K., Yang, Z., Shao, Y., Liu, L., & Zhang, F. (2016). Rice phenology retrieval automatically using

polarimetric SAR. *International Geoscience and Remote Sensing Symposium (IGARSS)*, *2016-November*, 5674–5677. https://doi.org/10.1109/IGARSS.2016.7730482

Lopez-Sanchez, J. M., Cloude, S. R., & Ballester-Berman, J. D. (2012). Rice phenology monitoring by means of SAR polarimetry at X-band. *IEEE Transactions on Geoscience and Remote Sensing*, *50*(7 PART 2), 2695–2709. https://doi.org/10.1109/TGRS.2011.2176740

Ma, G., Zhao, Q., Wang, Q., & Liu, M. (2018). On the Effects of InSAR Temporal Decorrelation and Its Implications for Land Cover Classification: The Case of the Ocean-Reclaimed Lands of the Shanghai Megacity. *Sensors (Basel, Switzerland)*, *18*(9). https://doi.org/10.3390/S18092939

Mahan, M. Y., Chorn, C. R., & Georgopoulos, A. P. (2015). White Noise Test: detecting autocorrelation and nonstationarities in long time series after ARIMA modeling. *PROC. OF THE 14th PYTHON IN SCIENCE CONF*. https://doi.org/10.25080/Majora-7b98e3ed-00f

Mandal, D., Kumar, V., Bhattacharya, A., Rao, Y. S., Siqueira, P., & Bera, S. (2018). Sen4Rice: A processing chain for differentiating early and late transplanted rice using time-series sentinel-1 SAR data with google earth engine. *IEEE Geoscience and Remote Sensing Letters*, *15*(12), 1947–1951. https://doi.org/10.1109/LGRS.2018.2865816

Martinis, S., Rieke, C., J-P Schumann, G., Balzter, H., & Thenkabail, P. S. (2015). Backscatter Analysis Using Multi-Temporal and Multi-Frequency SAR Data in the Context of Flood Mapping at River Saale, Germany. *Remote Sensing 2015, Vol. 7, Pages 7732-7752*, *7*(6), 7732–7752. https://doi.org/10.3390/RS70607732

Miralles, D. G., Crow, W. T., & Cosh, M. H. (2010). Estimating Spatial Sampling Errors in Coarse-Scale Soil Moisture Estimates Derived from Point-Scale Observations. *Journal of Hydrometeorology*, *11*(6), 1423–1429. https://doi.org/10.1175/2010JHM1285.1

Moore, D. S., & McCabe, G. P. (1999). *Introduction to the practice of statistics*. W.H. Freeman. https://books.google.com/books/about/Introduction_to_the_Practice_of_Statisti.html?id=-_DEQgAACAAJ

Nasirzadehdizaji, R., Sanli, F. B., Abdikan, S., Cakir, Z., Sekertekin, A., & Ustuner, M. (2019). Sensitivity Analysis of Multi-Temporal Sentinel-1 SAR Parameters to Crop Height and Canopy Coverage. *Applied Sciences 2019, Vol. 9, Page 655*, *9*(4), 655. https://doi.org/10.3390/APP9040655

Nguyen, D. B., Gruber, A., & Wagner, W. (2016). Mapping rice extent and cropping scheme in the Mekong Delta using Sentinel-1A data. *Http://Dx.Doi.Org/10.1080/2150704X.2016.1225172*, *7*(12), 1209–1218. https://doi.org/10.1080/2150704X.2016.1225172

Nilsson, C., Jansson, R., & Zinko, U. (1997). Long-term responses of river-margin vegetation to water-level regulation. *Science*, *276*(5313), 798–800. https://doi.org/10.1126/SCIENCE.276.5313.798/ASSET/0A192D32-1F51-453C-A4DE-270D6F929FF8/ASSETS/GRAPHIC/SE1675058001.JPEG

Palacios-Orueta, A., Huesca, M., Whiting, M. L., Litago, J., Khanna, S., Garcia, M., & Ustin, S. L. (2012). Derivation of phenological metrics by function fitting to time-series of Spectral Shape Indexes AS1 and AS2: Mapping cotton phenological stages using MODIS time series. *Remote Sensing of Environment*, *126*, 148–159. https://doi.org/10.1016/J.RSE.2012.08.002

Pang, J., Zhang, R., Yu, B., Liao, M., Lv, J., Xie, L., Li, S., & Zhan, J. (2021). Pixel-level rice planting information monitoring in Fujin City based on time-series SAR imagery. *International Journal of Applied Earth Observation and Geoinformation*, *104*, 102551. https://doi.org/10.1016/J.JAG.2021.102551

Phan, H., Toan, T. Le, & Bouvet, A. (2021). Understanding Dense Time Series of Sentinel-1 Backscatter from Rice Fields: Case Study in a Province of the Mekong Delta, Vietnam. *Remote Sensing 2021, Vol. 13, Page 921*, *13*(5), 921. https://doi.org/10.3390/RS13050921

Philippine Statistics Authority. (2021, February 17). *Domestic wholesale price of palay in the Philippines from 2012*

to 2021 (per kilogram in Philippine pesos) [Graph]. Statista. https://www.statista.com/statistics/1046657/philippines-domestic-wholesale-price-palay-rice/

Plotnikov, D., Kolbudaev, P., Matveev, A., Loupian, E., & Proshin, A. (2022). Daily surface reflectance reconstruction using LOWESS on the example of various satellite systems. *2022 8th International Conference on Information Technology and Nanotechnology, ITNT 2022*. https://doi.org/10.1109/ITNT55410.2022.9848630

Potin, P., Rosich, B., Grimont, P., Miranda, N., Shurmer, I., O'Connell, A., Krassenburg, M., & Torres, R. (2016). Sentinel-1 Mission Status. *Proceedings of EUSAR 2016: 11th European Conference on Synthetic Aperture Radar*, 1–6. https://qc.sentinel1.eo.esa.int/

Pouliot, D., Latifovic, R., & Olthof, I. (2008). Trends in vegetation NDVI from 1 km AVHRR data over Canada for the period 1985–2006. *Http://Dx.Doi.Org/10.1080/01431160802302090*, *30*(1), 149–168. https://doi.org/10.1080/01431160802302090

Sakamoto, T., Yokozawa, M., Toritani, H., Shibayama, M., Ishitsuka, N., & Ohno, H. (2005). A crop phenology detection method using time-series MODIS data. *Remote Sensing of Environment*, *96*(3–4), 366–374. https://doi.org/10.1016/J.RSE.2005.03.008

Schloss, P. D. (2018). Identifying and Overcoming Threats to Reproducibility, Replicability, Robustness, and Generalizability in Microbiome Research. *MBio*, *9*(3). https://doi.org/10.1128/MBIO.00525-18

Schlund, M., & Erasmi, S. (2020). Sentinel-1 time series data for monitoring the phenology of winter wheat. *Remote Sensing of Environment*, *246*, 111814. https://doi.org/10.1016/J.RSE.2020.111814

Schwarcz, P., Mura, L., Pätoprstý, M., & Schwarczová, L. (2012). The impact of employment in agriculture on overall employment and development: a case study of the district of Topol'čany, Slovakia. *SEER: Journal for Labour and Social Affairs in Eastern Europe*, *15*(4), 483–492. http://www.jstor.org/stable/43293489

Seck, P. A., Diagne, A., Mohanty, S., & Wopereis, M. C. S. (2012). Crops that feed the world 7: Rice. *Food Security 2012 4:1*, *4*(1), 7–24. https://doi.org/10.1007/S12571-012-0168-1

Stasolla, M., & Neyt, X. (2018). An Operational Tool for the Automatic Detection and Removal of Border Noise in Sentinel-1 GRD Products. *Sensors 2018, Vol. 18, Page 3454*, *18*(10), 3454. https://doi.org/10.3390/S18103454

Statista. (2022). • *Rice consumption by country 2019 | Statista*. https://www.statista.com/statistics/255971/top-countries-based-on-rice-consumption-2012-2013/

Statista Research Department. (2021). *Agriculture in the Philippines - statistics & facts* . https://www.statista.com/topics/5744/agriculture-industry-in-the-philippines/#dossierKeyfigures

Steffany, S., Granada, B., & Ongy, E. E. (2017). Optimization of Farm Income of Communities Vulnerable to Climate Change Conditions. *Journal of Society and Technology*, *7*(1), 88–100. http://www.jst-online.org/index.php/JST/article/view/123

Suwannachatkul, S., Kasetkasem, T., Chumkesornkulkit, K., Rakwatin, P., Chanwimaluang, T., & Kumazawa, I. (2014). *Rice Cultivation and Harvest Date Estimation Using MODIS NDVI Time-series Data.*

Thies, B., & Bendix, J. (2011). Satellite based remote sensing of weather and climate: recent achievements and future perspectives. *Meteorological Applications*, *18*(3), 262–295. https://doi.org/10.1002/MET.288

Torbick, N., Chowdhury, D., Salas, W., Qi, J., Baghdadi, N., Li, X., & Thenkabail, P. S. (2017). Monitoring Rice Agriculture across Myanmar Using Time Series Sentinel-1 Assisted by Landsat-8 and PALSAR-2. *Remote Sensing 2017, Vol. 9, Page 119*, *9*(2), 119. https://doi.org/10.3390/RS9020119

Torres, R., Navas-Traver, I., Bibby, D., Lokas, S., Snoeij, P., Rommen, B., Osborne, S., Ceba-Vega, F.,

Potin, P., & Geudtner, D. (2017). Sentinel-1 SAR system and mission. *2017 IEEE Radar Conference, RadarConf 2017*, 1582–1585. https://doi.org/10.1109/RADAR.2017.7944460

Tsyganskaya, V., Martinis, S., & Marzahn, P. (2019). Flood Monitoring in Vegetated Areas Using Multitemporal Sentinel-1 Data: Impact of Time Series Features. *Water 2019, Vol. 11, Page 1938*, *11*(9), 1938. https://doi.org/10.3390/W11091938

Turner, A. P., Jackson, J. J., Sama, M. P., & Montross, M. D. (2021). Impact of Delayed Harvest on Corn Yield and Harvest Losses. *Applied Engineering in Agriculture*, *37*(4), 595–604. https://doi.org/10.13031/AEA.14561

Ullmann, T., Jagdhuber, T., Hoffmeister, D., May, S. M., Baumhauer, R., & Bubenzer, O. (2023). Exploring Sentinel-1 backscatter time series over the Atacama Desert (Chile) for seasonal dynamics of surface soil moisture. *Remote Sensing of Environment*, *285*, 113413. https://doi.org/10.1016/J.RSE.2022.113413

United Nations. (2016). *Goal 2: Zero Hunger - United Nations Sustainable Development*. https://www.un.org/sustainabledevelopment/hunger/

United Nations. (2019). *World Population Prospects 2019: Highlights | Multimedia Library - United Nations Department of Economic and Social Affairs*. https://www.un.org/development/desa/publications/world-population-prospects-2019-highlights.html

Veloso, A., Mermoz, S., Bouvet, A., Le Toan, T., Planells, M., Dejoux, J. F., & Ceschia, E. (2017). Understanding the temporal behavior of crops using Sentinel-1 and Sentinel-2-like data for agricultural applications. *Remote Sensing of Environment*, *199*, 415–426. https://doi.org/10.1016/J.RSE.2017.07.015

Vicente-Guijalba, F., Martinez-Marin, T., & Lopez-Sanchez, J. M. (2014). Crop phenology estimation using a multitemporal model and a kalman filtering strategy. *IEEE Geoscience and Remote Sensing Letters*, *11*(6), 1081–1085. https://doi.org/10.1109/LGRS.2013.2286214

Vreugdenhil, M., Wagner, W., Bauer-Marschallinger, B., Pfeil, I., Teubner, I., Rüdiger, C., & Strauss, P. (2018). Sensitivity of Sentinel-1 Backscatter to Vegetation Dynamics: An Austrian Case Study. *Remote Sensing 2018, Vol. 10, Page 1396*, *10*(9), 1396. https://doi.org/10.3390/RS10091396

Walls, T., Wilson, M., Madsen, D., Jensen, M., Sullivan, S., Thomas, A., Walls, J., Wilson, M. L., Addario, M., Hally, I., & Walls, T. J. (2014). Multi-mission, autonomous, synthetic aperture radar. *In Radar Sensor Technology XVIII*, *9077*(907706), SPIE. https://doi.org/10.1117/12.2053561

Wang, J., Huang, J. feng, Wang, X. zhen, Jin, M. ting, Zhou, Z., Guo, Q. ying, Zhao, Z. wen, Huang, W. jiao, Zhang, Y., & Song, X. dong. (2015). Estimation of rice phenology date using integrated HJ-1 CCD and Landsat-8 OLI vegetation indices time-series images. *Journal of Zhejiang University: Science B*, *16*(10), 832–844. https://doi.org/10.1631/JZUS.B1500087/TABLES/5

Wong, T. T., & Yeh, P. Y. (2020). Reliable Accuracy Estimates from k-Fold Cross Validation. *IEEE Transactions on Knowledge and Data Engineering*, *32*(8), 1586–1594. https://doi.org/10.1109/TKDE.2019.2912815

Yang, W., Peng, S., Laza, R. C., Visperas, R. M., & Dionisio-Sese, M. L. (2008). Yield Gap Analysis between Dry and Wet Season Rice Crop Grown under High-Yielding Management Conditions. *Agronomy Journal*, *100*(5), 1390–1395. https://doi.org/10.2134/AGRONJ2007.0356

Yoshida, S. (1981). *Fundamentals of Rice Crop Science - Shouichi Yoshida - Google Boeken*. The International Rice Research Institute. https://books.google.nl/books?hl=nl&lr=&id=wS-teh0I5d0C&oi=fnd&pg=PP2&ots=VD1Dk__kZG&sig=Z4qi3rHahKMzQdNZS8B3-g-iOcM&redir_esc=y#v=onepage&q&f=false

8. APPENDICES

Appendix 1. Breusch-Godfrey test p-values for Leyte rice fields during the dry season

Field number	VH (p-values)	VV p-values	VH/VV p-values
801	<0.05	<0.05	<0.05
802	<0.05	<0.05	<0.05
804	<0.05	<0.05	<0.05
805	<0.05	**>0.05**	<0.05
806	<0.05	<0.05	<0.05
808	<0.05	**>0.05**	<0.05
809	<0.05	<0.05	<0.05
810	<0.05	**>0.05**	<0.05
811	<0.05	<0.05	<0.05
812	<0.05	<0.05	<0.05
813	<0.05	<0.05	<0.05
814	<0.05	<0.05	<0.05
815	<0.05	<0.05	<0.05
816	<0.05	<0.05	<0.05
817	<0.05	<0.05	<0.05
821	<0.05	<0.05	<0.05
822	<0.05	<0.05	<0.05
823	<0.05	<0.05	<0.05
825	<0.05	<0.05	<0.05
826	<0.05	<0.05	<0.05
827	<0.05	<0.05	<0.05
828	<0.05	<0.05	<0.05
829	<0.05	<0.05	<0.05
830	<0.05	<0.05	<0.05
832	<0.05	<0.05	<0.05
835	<0.05	<0.05	<0.05
837	<0.05	<0.05	<0.05
842	<0.05	<0.05	<0.05
843	**>0.05**	**>0.05**	<0.05
844	<0.05	<0.05	<0.05
845	<0.05	<0.05	<0.05
846	<0.05	**>0.05**	<0.05
847	<0.05	<0.05	<0.05
848	<0.05	<0.05	<0.05
849	<0.05	<0.05	<0.05
850	<0.05	<0.05	<0.05
851	<0.05	<0.05	<0.05
852	<0.05	<0.05	<0.05
853	<0.05	<0.05	<0.05
855	<0.05	<0.05	<0.05
856	<0.05	<0.05	<0.05
857	<0.05	<0.05	<0.05

Appendix 2. Comparison between field information and detected dates

	Polarization	Farmer-reported TD vs Detected TD	Farmer-reported HD vs Detected HD
Agusan del Sur (dry season)	VH	15/19 (78.95%) Mean difference: -10 days Median difference: -10 days RMSD: **12.4 days** Mean absolute difference: 10 days	16/19 (84.21%) Mean difference: -11 days Median difference: -10 days RMSD: 17.5 days Mean absolute difference: 11 days
	VV	16/19 (84.21%) Mean difference: -5 days Median difference: -7 days RMSD: **9.2 days** Mean absolute difference: 7 days	16/19 (84.21%) Mean difference: -10 days Median difference: -6 days RMSD: 24.3 days Mean absolute difference: 18 days
	VH/VV	19/19 (100%) Mean difference: -21 days Median difference: -17 days RMSD: 23.9 days Mean absolute difference: 20 days	18/19 (94.74%) Mean difference: 2 days Median difference: 3 days RMSD: 17.6 days Mean absolute difference: 15 days
Agusan del Sur (wet season)	VH	17/19 (89.47%) Mean difference: -3 days Median difference: -2 days RMSD: 28 days Mean absolute difference: 28 days	11/19 (57.89%) Mean difference: -15 days Median difference: -13 days RMSD: 16.3 days Mean absolute difference: 13 days
	VV	16/19 (84.21%) Mean difference: -38 days Median difference: -46 days RMSD: 45 days Mean absolute difference: 37 days	12/19 (63.16%) Mean difference: -5 days Median difference: -16 days RMSD: 29 days Mean absolute difference: 25 days
	VH/VV	13/19 (68.42%) Mean difference: -9 days Median difference: -9 days RMSD: **14 days** Mean absolute difference: 12 days	13/19 (68.42%) Mean difference: 4 days Median difference: 6 days RMSD: **8 days** Mean absolute difference: 8 days
Cagayan (dry season)	VH	33/38 (86.84%) Mean difference: -13 days Median difference: -12 days RMSD: 21 days Mean absolute difference: 13 days	35/38 (92.11%) Mean difference: 11 days Median difference: 15 days RMSD: 23 days Mean absolute difference: 17 days
	VV	19/38 (50%) Mean difference: -18 days Median difference: -13 days RMSD: 38 days Mean absolute difference: 30 days	20/38 (52.63%) Mean difference: 25 days Median difference: 30 days RMSD: 39 days Mean absolute difference: 30 days
	VH/VV	30/38 (78.95%) Mean difference: -13 days Median difference: -13 days RMSD: **16 days** Mean absolute difference: 13 days	33/38 (86.84%) Mean difference: 0 days Median difference: 3 days RMSD: **16 days** Mean absolute difference: 15 days
Cagayan (wet season)	VH	34/38 (89.47%) Mean difference: -25 days Median difference: -21 days RMSD: 30 days Mean absolute difference: 20 days	32/38 (84.21%) Mean difference: -13 days Median difference: -11 days RMSD: 19 days Mean absolute difference: 13 days
	VV	28/38 (73.68%) Mean difference: -60 days Median difference: -60 days	28/38 (73.68%) Mean difference: -28 days Median difference: -27 days

		RMSD: 61 days Mean absolute difference: 59 days	RMSD: 33 days Mean absolute difference: 26 days
	VH/VV	32/38 (84.21%) Mean difference: -23 days Median difference: -18 days RMSD: 29 days Mean absolute difference: 24 days	31/38 (81.58%) Mean difference: 0 days Median difference: 1 days RMSD: **14 days** Mean absolute difference: 11 days
Leyte (dry season)	VH	36/42 (85.71%) Mean difference: 2 days Median difference: 3 days RMSD: **13.7 days** Mean absolute difference: 9 days	31/42 (73.81%) Mean difference: -10 days Median difference: -11 days RMSD: 17.5 days Mean absolute difference: 11 days
	VV	33/42 (78.57%) Mean difference: 5 days Median difference: 7 days RMSD: **13.6 days** Mean absolute difference: 10 days	34/42 (80.95%) Mean difference: -11 days Median difference: -11 days RMSD: 17.4 days Mean absolute difference: 13 days
	VH/VV	37/42 (88.10%) Mean difference: -22 days Median difference: -24 days RMSD: 25 days Mean absolute difference: 21 days	20/42 (47.62%) Mean difference: -2 days Median difference: 3 days RMSD: **16 days** Mean absolute difference: 13 days
Leyte (wet season)	VH	39/42 (92.86%) Mean difference: -21 days Median difference: -21 days RMSD: 27 days Mean absolute difference: 21 days	30/42 (71.43%) Mean difference: -15 days Median difference: -14 days RMSD: 25 days Mean absolute difference: 17 days
	VV	34/42 (80.95%) Mean difference: -32 days Median difference: -34 days RMSD: 36 days Mean absolute difference: 32 days	23/42 (54.76%) Mean difference: 3 days Median difference: -1 days RMSD: 22 days Mean absolute difference: 16 days
	VH/VV	33/42 (78.57%) Mean difference: -28 days Median difference: -28 days RMSD: 30 days Mean absolute difference: 27 days	39/42 (92.86%) Mean difference: -1 days Median difference: -5 days RMSD: 22 days Mean absolute difference: 18 days

Appendix 3. Maps showing the temporal difference between the farmer-reported and detected dates in Agusan del Sur for VH polarization during the dry season

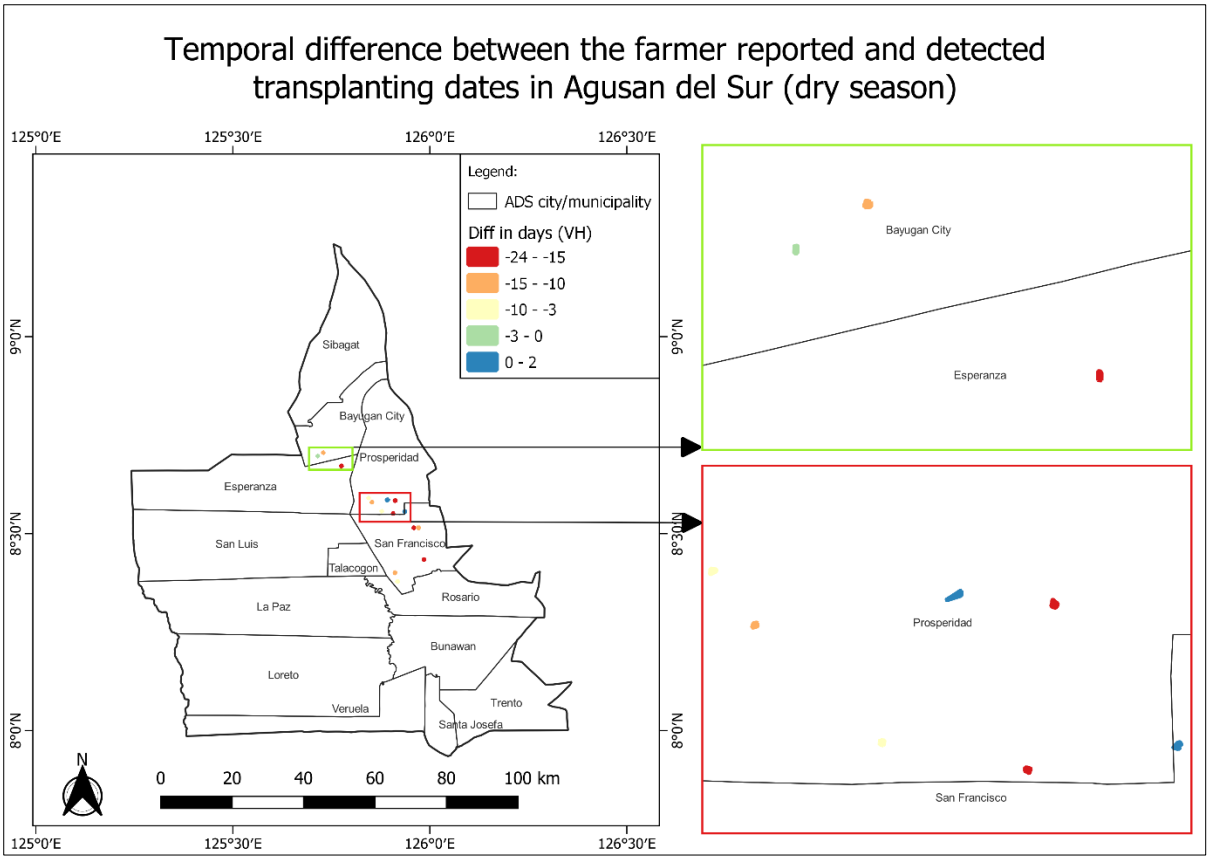

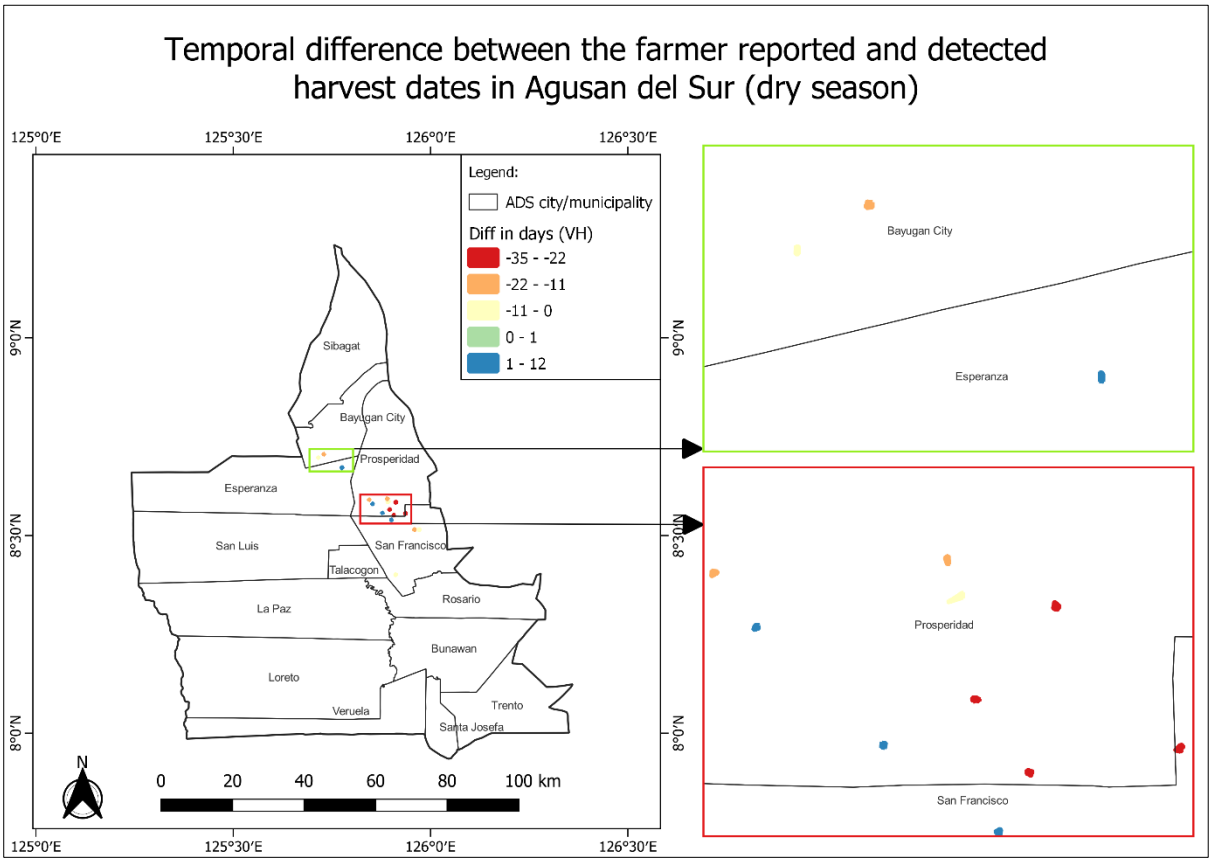

Appendix 4. Maps showing the temporal difference between the farmer-reported and detected dates in Cagayan for VH/VV polarization during the dry season